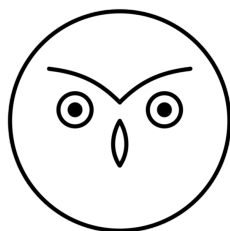


# The Cuban Scientist

Year 2020

Volume 1 | Issue 1





# THE CUBAN SCIENTIST

Volume 1, Issue 1

June 30, 2020

We are extremely pleased to launch the first issue of THE CUBAN SCIENTIST (TCS), with articles covering subjects from the natural, social and medical sciences, engineering and technology.

Initially a small group of Cuban scientists working in different locations, we started considering the idea of a scientific review magazine focused on the broader Cuban scientific community. It had become clear to us that there is a lot of science ‘made by Cubans’ that we as Cuban scientists are not aware of; especially beyond each one’s area of research but sometimes within it as well.

By the end of 2019 this idea crystallized into TCS: *an online journal where Cuban scientists from all branches of science and technology, working inside or outside Cuba, can share their research results with the community in the form of two-page reports, summarizing works already published in peer-reviewed journals.*

An important point is that we interpret ‘Cuban’ in an inclusive way, comprising all the scientists who identify themselves with this community, regardless of their place of birth or where they live.

TCS’s mission is to establish and strengthen ties among Cuban scientists by contributing to their self-awareness as a community, fostering collaboration and facilitating knowledge-sharing. It aims to serve as a free information layer bypassing geographical and institutional barriers. Our goal is that TCS one day becomes *the* reference point for ‘science made by Cubans’.

We want to thank all those who made this first issue possible and take the opportunity to encourage other scientists to publish their work with us, for the benefit of our scientific community.

In this issue:

**Cuban Sci. 2020, 1(1): 1–2** — Natural Sciences

*FIRA: Rapid Manufacture of High-efficiency Perovskite Solar Cells*

Sandy Sanchez

**Cuban Sci. 2020, 1(1): 3–4** — Natural Sciences

*A Monte Carlo from Belén*

Rogelio Díaz-Méndez

**Cuban Sci. 2020, 1(1): 5–6** — Social Sciences

*From Ancient Greeks to Modern Teaching*

Aris Quintana Nedelcos

**Cuban Sci. 2020, 1(1): 7–8** — Social Sciences

*Epistemological Beliefs and Metacognitive Strategies in Cuban University Students*

Maybí Morell

**Cuban Sci. 2020, 1(1): 9–10** — Natural Sciences

*An Entropic-Energetic View for the Dynamics of HIV Infection*

Ramon E. R. Gonzalez

**Cuban Sci. 2020, 1(1): 11–12** — Engineering and Technology

*Degradation of Two Chlorinated Pesticides Using Advanced Oxidation Processes*

Germán Cruz González, Carine Julcour, Sarra Gaspard and Ulises Jáuregui Haza

**Cuban Sci. 2020, 1(1): 13–14** — Natural Sciences

*Evaluation of the Molecular Inclusion Process of Organochlorine Pesticides at Cyclodextrins*

Anthuan Ferino-Pérez, Juan José Gamboa-Carballo and Ulises Jáuregui Haza

**Cuban Sci. 2020, 1(1): 15–16** — Social Sciences

*Network of scientific collaboration of Cuban researchers working in Europe: Perspective for the home country*

Miriam Palacios-Callender

**Cuban Sci. 2020, 1(1): 17–18** — Social Sciences

*MEMBIOSIM: a Submerged Membrane Bioreactor simulator for teaching its functioning*

Yusmel González Hernández, Ulises Jáuregui Haza, Claire Albasi and Marion Alliet

**Cuban Sci. 2020, 1(1): 19–20** — Natural Sciences

*Novel HIV matrix shell structure and potential functions*

Marcelo Marcet-Palacios

**Cuban Sci. 2020, 1(1): 21–22** — Natural Sciences

*Molecular modeling of chlordecone interactions with acidic activated carbons*

Kenia Melchor Rodríguez, Juan José Gamboa Carballo, Anthuan Ferino Pérez, Nady

Passe-Coutrin, Sarra Gaspard and Ulises Jáuregui Haza

**Cuban Sci. 2020, 1(1): 23–24** — Engineering and Technology

*Small bubbles and bubble bags: a scientific knowledge valorisation*

David Fernandez Rivas

**Cuban Sci. 2020, 1(1): 25–26** — Medical and Health Sciences

*A quantum vaccinomics approach to vaccine development*

José de la Fuente, Marinela Contreras, Sara Artigas-Jerónimo and Margarita Villar

**Cuban Sci. 2020, 1(1): 27–28** — Natural Sciences

*Gershgorin radii as natural bounds for the correlation energies*

A. Odriazola

# FIRA: Rapid Manufacture of High-efficiency Perovskite Solar Cells

Sandy Sanchez<sup>a1</sup>

<sup>1</sup>Adolphe Merkle Institute, University of Fribourg, Chemin des Verdiers 4, 1700 Fribourg, Switzerland

*We describe FIRA, a new method to manufacture solar cells. Its main advantages are its quick implementation and the high-efficiency of the resulting devices.*

Several antisolvent-free methods have been proposed to control perovskite film crystallization, resulting in perovskite solar cells (PSCs) with relatively high PCEs [1]. For example, Nie et al. demonstrated a hot-casting technique to grow continuous, pinhole-free perovskite films with millimeter-scale crystalline grains [2]. This method uses a hot ( $\sim 70$  °C) solution of lead iodide and methylamine hydrochloride spin-coated onto a hot (180 °C) substrate. This technique allowed the fabrication of planar solar cells with average (not stabilized) efficiencies approaching 16%. Li et al. proposed a vacuum-assisted method for one-square-centimeter PSCs with a stabilized PCE of around 20% [3]. Nevertheless, the extension of PSCs towards a technology remains challenging because of the lack of a method allowing to produce large-area devices (100 square-centimeters or larger) with PCEs comparable to lab-scale devices.

Rapid thermal annealing methods have been successfully used to control the crystallization of inorganic semiconductors and to prepare large-area devices made of highly crystalline phase-continuous films [4]. Similar approaches have been explored for PSCs with promising results [2]. In this direction, Troughton et al. proposed a short exposure with a highly intense near-infrared radiation to crystallize perovskite films, potentially enabling the preparation of large-area PSCs with high efficiencies.

In 2018, flash infrared annealing (FIRA), an antisolvent-free method that can be used to prepare methylammonium lead iodide (MAPbI<sub>3</sub>) PSCs with stabilized power conversion efficiencies up to 18.3%, has been introduced for the first time [5]. Using this method, perovskite film crystallization is completed within 2 seconds plus 8 seconds remaining in the dark at low temperature on the FIRA camera to completely remove the solvent. Such a rapid crystallization results in micrometer-size crystal grains arranged in a dense perovskite film. FIRA allows the manufacture of large-area (100 cm<sup>2</sup>) perovskite films and large-area devices (1.4 cm<sup>2</sup> of active area). Note that FIRA does not warm the substrate and is thus compatible with low-temperature processing on plastic substrates, enabling in particular roll-to-roll printing.

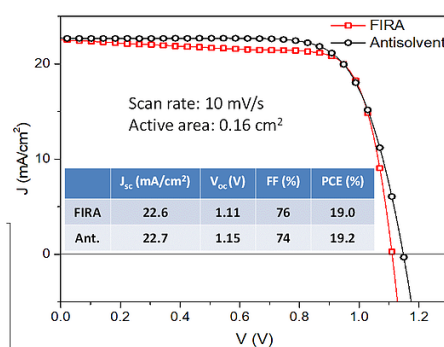


Figure 1: Current density-voltage (J-V) scans collected at 10 mV/s of two champion devices under 1.5 AM irradiation and the corresponding photovoltaic performance parameters.

## Photovoltaic performance of a PSC

The current density-voltage (J-V) curves and the corresponding device performance parameters for the two champion cells are shown in Figure 1. The FIRA-annealed PSCs exhibit a slightly higher fill factor (FF) and lower open circuit voltage ( $V_{oc}$ ) than the champion device made using the antisolvent method, while the short circuit currents ( $J_{sc}$ ) are similar. Note that the current density of the FIRA-device decreases between short circuit condition and 0.6 V forward bias, while it stays constant in the reference champion device. This is probably due to the fact the perovskite film is slightly too thick in the FIRA-device, compared to the ideal thickness of 500 nm as optimized for the antisolvent method. This results in a slightly higher series resistance, the absence of which would enhance the fill-factor even more.

## FIRA as a method to scale-up the manufacture of perovskite

Foreseeing the commercialization of PSCs, Figure 2 shows a scheme of a possible roll-to-roll production method employing FIRA to crystallize the perovskite film. The perovskite precursor solution can be deposited on the substrate using any of the roll-to-roll compatible methods available on the market [4], such as doctor-blading, slot-casting, spray-coating, screen-printing and inject-printing. The deposited film is then passed through the FIRA box which enables rapid

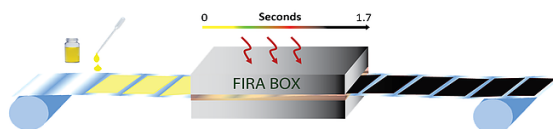


Figure 2: Scheme of a roll-to-roll production line for perovskite thin films crystallized within 2 seconds using FIRA.

(within 2 seconds) perovskite film crystallization.

### Summary

We demonstrate FIRA as a new method to prepare state-of-the-art efficiency perovskite solar cells with a good reproducibility. The advantages of FIRA are: i. the elimination of the antisolvent to induce the perovskite film crystallization, which drastically reduces the use of organic solvent in the PSC manufacture, making the process environmental more friendly; ii. FIRA is compatible with large area device manufacture and flexible substrates which require low temperature processing; iii. FIRA is suitable for fast throughput production lines, such as roll-to-roll deposition

methods.

### Notes

a. Email: sandysanche@gmail.com

### References

- [1] W. Nie, H. Tsai, R. Asadpour, J.-C. Blancon, A. J. Neukirch, G. Gupta, J. J. Crochet, M. Chhowalla, S. Tretiak, M. A. Alam, H.-L. Wang and A. D. Mohite, *Science* **347** (2015) 522-525.
- [2] J. Xu, Z. Hu, X. Jia, L. Huang, X. Huang, L. Wang, P. Wang, H. Zhang, J. Zhang, J. Zhang and Y. Zhu, *Organic Electronics* **34** (2016) 84-90.
- [3] J. Troughton, C. Charbonneau, M. J. Carnie, M. L. Davies, D. A. Worsley and T. M. Watson, *Journal of Materials Chemistry A* **3** (2015) 9123-9127.
- [4] K. Hwang, Y.-S. Jung, Y.-J. Heo, F.H. Scholes, S. E. Watkins, J. Subbiah, D. J. Jones, D.-Y. Kim and D. Vak, *Advanced Materials* **27** (2015) 1241-1247.
- [5] S. Sanchez, X. Hua, N. Phung, U. Steiner and A. Abate, *Advanced Energy Materials* **8** (2018) 1702915.

# A Monte Carlo from Belén

Rogelio Díaz-Méndez<sup>a1</sup>

<sup>1</sup>Department of Physics, KTH - Royal Institute of Technology, 10691 Stockholm, Sweden

*The Event-Driven Monte Carlo algorithm is introduced. It applies to problems with discrete degrees of freedom, accurately finding the temporal evolution at all time scales.*

Back in 2010, when now Prof. Alejandro Mendoza-Coto was a master student in Cuba, we stumbled on the fact that, to the best of our knowledge, there were no numerical methods to study the dynamics of an Ising-like spin system in real, physical time. Not very aware of the current literature on Kinetic Monte Carlo (KMC) techniques, we started to consider the possibility of simulating single realizations of the master equation in one of the many discussions we had at my place, at the rooftop of an old building of the Belén neighborhood in Old Havana.

After many sessions, the general idea seemed to be very simple: the full system can be decomposed in a set of two-level subsystems containing all possible changes. Indeed, all the transitions the full system could immediately undergo from a state  $X$ , can be mapped as a set of  $N$  two-level “new systems” with energies corresponding to that of states  $X$  and  $Y_i$ , where  $Y_i$  is the final configuration for each possible change  $i \in [1, 2, \dots, N]$ . Thus, the immediate evolution of the full system in a state  $X$  can be studied by preparing  $N$  two-level subsystems in an initial state of energy  $E(X)$ , and letting them race for transition to the corresponding level  $E(Y_i)$ . The winner  $i = w$  will reset the whole configuration, so that we can make  $X = Y_w$  and start all over again. The project, nevertheless, got not too far from coffee talks and a bunch of useless formulas and code lines.

Five years later, we met in Strasbourg under the hosting of Prof. Guido Pupillo, who became interested in the potential of the original idea, particularly when addressing the very early stages of the dynamics. By that time we were quite familiar with KMC and time-quantified Monte Carlo methods, and could see more clearly the advantages of the Belén’s scheme. We realized that, despite several decades of improvement, no reliable numerical technique was capable of reproducing the master equation kinetics at very short times. So we finally designed and implemented what was eventually published with the name of Event-Driven Monte Carlo algorithm [1], applicable to all systems of discrete variables (like Ising spins), whose summarized flowchart is shown in Fig. 1.

For systems of discrete variables following stochastic evolution, the probability distribution  $\mathcal{P}(X, t)$  of being at a given state  $X$  at time  $t$  is given by the master equation

$$\frac{\partial \mathcal{P}(X, t)}{\partial t} = \sum_Y W(X|Y)\mathcal{P}(Y, t) - \sum_Y W(Y|X)\mathcal{P}(X, t) \quad (1)$$

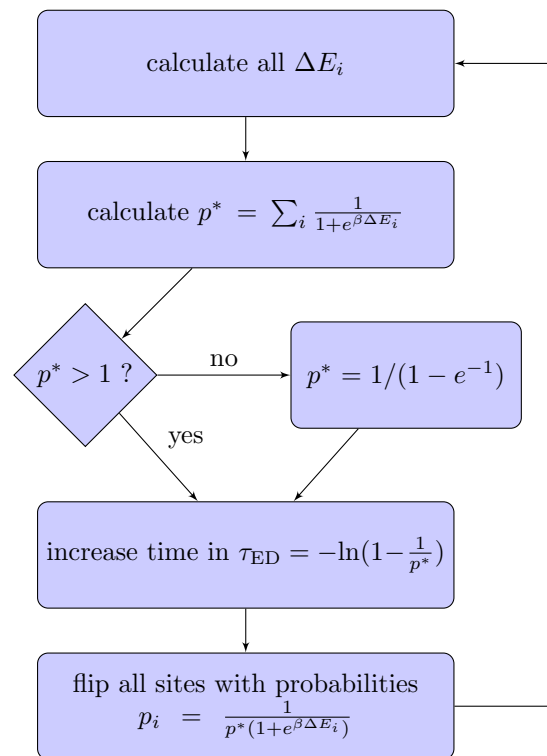


Figure 1: Flowchart for the elementary step of the Event-Driven algorithm. The energy difference  $\Delta E_i$  is associated to the flipping of spin  $i$  while all the rest are fixed, i.e. the energy differences between the two levels of the subsystems.

where  $W(Y|X)$  is the transition rate from state  $X$  to state  $Y$ . Let’s now consider the subsystems corresponding to state  $X$ . For single-spin-flip dynamics, each spin  $i$  defines a subsystem occupying the level  $o$ , while level  $f$ , corresponding to the spin flip, is initially free. So that if  $P_k^l(t)$  is the probability of subsystem  $k$  to be at the level  $l$  at a time  $t$ , then  $P_i^o(0) = 1$  and  $P_i^f(0) = 0$ . While no transition has occurred, the race can be described by  $N$  independent systems of two equations

$$\frac{dP_i^o(t)}{dt} = \Gamma_i^{fo} P_i^f(t) - \Gamma_i^{of} P_i^o(t) \quad (2)$$

$$\frac{dP_i^f(t)}{dt} = \Gamma_i^{of} P_i^o(t) - \Gamma_i^{fo} P_i^f(t) \quad (3)$$

where  $\Gamma_i^{of}$  and  $\Gamma_i^{fo}$  are the transition rates of the two-level subsystem associated to the flip of spin  $i$ . Imposing the Boltzmann occupation probabilities for the

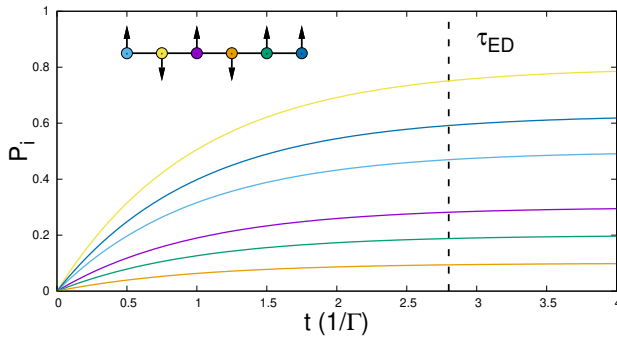


Figure 2: Schematic representation of  $P_i$  for a system of six spins marked with different colors. The interacting Hamiltonian (not shown) sets the prefactors  $P_i^f(\infty)$ .

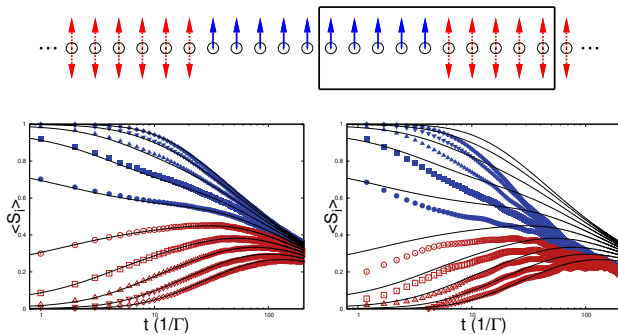


Figure 3: Top: Initial condition of a long Ising chain prepared with ten central spins in a ferromagnetic configuration; the black rectangle highlights the spins whose average magnetization is plotted below. Left: Average magnetization obtained with Event-Driven MC simulations. Right: Average magnetization obtained with KMC simulations. The solid black curves are the exact solution by R. J. Glauber [3].

infinite-time limit, and using the simple form of the partition function of the two-level subsystem, transition probabilities  $P_i(t)$  can be solved analytically to give

$$P_i(t) = P_i^f(t) = P_i^f(\infty) \left[ 1 - e^{-(\Gamma_i^{of} + \Gamma_i^{fo}) t} \right], \quad (4)$$

where  $P_i^f(\infty) = 1/[1 + e^{\beta(E_i^f - E^o)}]$ , and the unit of time can be taken to be the inverse of the characteristic frequency  $\Gamma = \Gamma_i^{of} + \Gamma_i^{fo}$  assumed as constant.

The probabilities of Eq. (4) are schematically shown in Fig. 2 for a finite chain of Ising-like spins interacting via some Hamiltonian. The goal then is to propose spin flips with these probabilities evaluated in some time  $\tau_{ED}$ , large enough to be useful but small enough to ensure that Eqs. (2) and (3) are still valid. This

is naturally guaranteed by imposing the normalization condition  $\sum_i P_i(\tau_{ED}) = 1$  and solving for  $\tau_{ED}$ , which leads to

$$\Gamma \tau_{ED} = -\ln [1 - P_*^{-1}], \quad (5)$$

where  $P_* = \sum_i P_i^f(\infty)$ . Thus defined, the time  $\tau_{ED}$  is such that, in average, only one spin has made the transition, and hence the full system is in a new state.

We compared the outcome of our algorithm with state-of-the-art implementations of the KMC schemes [2] by recording the local magnetization of a spin chain prepared in a known initial state. This is perhaps the most complex problem of discrete-variables in statistical physics for which an exact solution of the dynamics is known at all timescales [3].

In the top panel of Fig. 3 the initial condition of the ensemble of chains is represented with blue arrows for spins that start with  $\langle S_i \rangle = 1$  and red double arrows for spins starting with  $\langle S_i \rangle = 0$ . As can be seen from the lower panels, and unlike the KMC scheme, the results from the Event-Driven algorithm are in a pretty nice agreement with the exact solution for the local magnetization.

In summary, we found that the heuristic assumptions and phase-space constructions lying at the basis of KMC techniques are not good for studying times of the order of consecutive elementary events. In the context of ultrafast dynamics, the algorithm first discussed in Belén became perhaps the first one to reproduce the exact master equation along the time axis. The formulation of this Event-Driven MC can be made very general to attack any discrete variable problem. The only requirements are that i) the system can be decomposed into a set of  $N$  two-level subsystems, and ii) any dynamical evolution can be described by sequential transitions of these individual subsystems.

## Notes

a. Email: nep2n0@gmail.com

## References

- [1] A. Mendoza-Coto, R. Díaz-Méndez and G. Pupillo, Event-driven Monte Carlo: Exact dynamics at all time scales for discrete-variable models, *Europhysics Letters* **114** (2016) 50003
- [2] M. Leetmaa and N. V. Skorodumova, KMCLib: A general framework for lattice kinetic Monte Carlo (KMC) simulations, *Computer Physics Communications* **185** (2014) 2340
- [3] R. J. Glauber, Time-Dependent Statistics of the Ising Model, *Journal of Mathematical Physics* **4** (1963) 294

# From Ancient Greeks to Modern Teaching

Aris Quintana Nedelcos<sup>a1</sup>

<sup>1</sup>Department of Materials Science and Engineering, University of Sheffield, Mappin Street, Sheffield S1 3JD, UK

*Back during my time at the Universidad Tecnológica de La Habana “Jose Antonio Echeverría”, CUJAE I assist with a workshop on the Problem Base Learning (PBL) approach to teaching. Little did I know about the serious science behind the development of innovative Learning and Teaching approaches. Even less on how far in our history, it is possible to track our “modern” problems and solutions! In the present contribution I share with the readers some of these findings. I will particularly focus on those corresponding to the Hellenistic times of the classical Greco-Roman philosophy, and hopefully, just hopefully, I will be able to transmit how modern these “ancient thoughts” look like.<sup>b</sup>*

The concept of education denotes the methods by which a society maintains its knowledge, culture and values, and how it affects the physical, mental, emotional, moral and social aspects of the person.

The development of pedagogical thought took place in the classic Greco-Roman period (from the 7th century BC) with outstanding figures, such as Democritus, Quintilian, Socrates, Aristotle and Plato. The latter appears in history as the thinker who came to possess a true philosophy of education.

Today, different experiences have developed in a large number of countries and universities, which have been reported in the bibliography. They have tried to overcome the deficiencies of the traditional teaching system, by introducing new pedagogical models. They base their success on the use of cognitive processes, inherent in the human beings, in favor for the learning process by the student.

The significant increase in enrollment within universities, the heterogeneity of new admissions, the increasingly deficient general preparation of undergraduates, and the professional skills that industry demands from alumni, are some of the factors that motivate and demand a change in the educational system.

This work tries to show how the fundamental bases of some of the “new” and successful educational models, can be found from the first philosophical ideas developed by the great Greek thinkers, and maintained during the later history.

For example, the dialectic, developed by Zeno of Elea (495-430 BC) as member of the pre-Socratic Eleatic school, where the results of the abstract argumentation were given more importance than the testimonies of the senses (epistemological rationalism).

Socrates (470-399 BC) tried to make from philosophy a science. For this, he defended the inductive method and condemned the deductive method of the pre-Socratics. He didn't accept the universal truth as the ground that support every knowledge. But, rather he would experimentally observe the concrete reality and, in any case, induce, from here, laws or general principles [1].

Socrates develops a practical method based on the

dialogue, on the conversation: “Dialectics”, in which through inductive reasoning one could hope to achieve the universal definition of the terms under investigation. This method consisted of two phases: irony and maieutic. In the first phase, the fundamental objective is, through the practical analysis of concrete definitions, to recognize our ignorance on the definition we are looking for. Only with our ignorance recognized we are in the position to seek the truth. The second phase aims to bring a person's latent ideas into clear consciousness, by eliciting new ideas from another [2]. The Socratic dialectic progressed from more incomplete or less adequate definitions to more complete or more adequate definitions until reaching the universal definition [3]. Although he did not write any work, his thinking has exerted an influence that still lasts. Immediately after his death, his disciples founded various schools. And while all of them recognized Socrates as initiator, each interpreted the master's teachings in a different way, sometimes even giving rise to incompatible ideas.

Plato (427-347 BC) appropriately perceived that there is a need to know what it is that one wants to teach and what one wants to prepare others for [4]. That, it cannot be assumed that someone already has the knowledge to be taught. Therefore, more knowledge is usually needed and, needed to be created. The really different in Plato's concept is the union between teaching with research, or between the professional skills standards with the principles of scientific knowledge. This is the originality of his theory for “Higher Education” set forth in The Republic. Thus, we are strongly tempted to believe that it was the attempt to achieve that, which led him to undertake the founding of The Academy.

Without a doubt, Plato's main disciple was Aristotle (384-322 BC), who argues that the natural quality of the intellect is not knowledge itself, but merely the faculty of acquiring knowledge.

For him, science was the result of building more complex reasoning systems. As has been pointed out in his logic, Aristotle distinguished between dialectic and analytic. For him, the dialectic only checks opinions for

their logical consistency. Analytics, on the other hand, works deductively based on principles that rest on experience and precise observation [4].

It was the Arabs, with exponents such as Al-Kindi (801-873), Al-Farabi (872-950) and Avicenna (980-1037) who rediscovered Aristotle and passed on to the scholastic philosophy that dominated teaching in the medieval universities in Europe from about 1100 to 1700. Later, during the European Renaissance of the 15th and 16th centuries his philosophy was overshadowed by new scientific concepts, but its influence, although no longer in physics, continued to be valid in philosophical thought in the strict sense in all the great thinkers such as in Leibniz, Hegel, etc.

In classic Rome, the moral, civil and religious education has a history of its own, while school instruction in a technical sense, especially with regard to Arts and Letters, is almost entirely Greek. The teaching at school was obsessive and repetitive, the “tamer” teacher spoke and the students repeated: most of the teaching was based on a memory logic [1].

In Rome, the birth of a critical conscience about school and education [1] was formed.

- Encolpius (The Satyricon, Petronious, 27 – 66 AD) said: “the boys at school become cretins, because they don’t see any of the things they practice in life”.
- Seneca (4 BC – 65 AD) observed that: “the necessary things are not learned by virtue of learning the useless ones”.

Back to “modern times”, in traditional universities, science is not always taught in a way that helps the student appropriate physical concepts and develop cognitive skills. The classical lecture method, assumes that the student must clearly accept the knowledge taught by the teacher [5]. Traditional education offers very little inductive reasoning and opportunities to help activate the processes of abstraction and generalization [6].

We have seen since the end of the 19th century (Sarmiento: 1811-1888, Spencer: 1820-1903, Tolstoi: 1828-1910) emerging theories that enhance the learning

process, based on cognitive learning processes, increasing the participation of the student as an active subject in their own education. The idea also arises that young people should not only be trained as a competent professional, enhancing skills according to the requirements of the profession. We also have a social duty, by forming a critical attitude that allows a global vision, it is recognized that in the process of education, the relationships between educator-educator are political, so we are also forming their position on life [7].

### Notes

- a. Email: a.quintana-nedelcos@sheffield.ac.uk
- b. Original version of this article is Ref. [8]

### References

- [1] M. González García, *Historia de la Educación, Maestría en educación*, Universidad Abierta de San Luis Potosí (2001).
- [2] R. Mondolfo, *Socrates*, Buenos Aires: Eudeba (1996).
- [3] J. Hirschberger, *Historia de la Filosofía*, Barcelona: Herder (1985).
- [4] M. Alighiero Manacorda, *Historia de la educación 1, de la antigüedad al 1500*, Mexico D.F.: Siglo Veintiuno, 2<sup>a</sup> Edición (1992).
- [5] P. Van Heuvelen, Learning to think like a physicist: A review of research-based instructional strategies, *American Journal of Physics*, **59** (1991) 891-897.
- [6] L. C. McDermott, What we teach and what is learned - closing the gap, *American Journal of Physics*, **59** (1991) 301-315.
- [7] P. Freire, *Pedagogía de la autonomía*, Mexico D.F.: Siglo Veintiuno (2004).
- [8] A. Quintana-Nedelcos and J. J. Llovera-González, La construcción del conocimiento como proceso activo en la enseñanza, *Latin-American Journal of Physics Education* **3** (2009) 19.

# Epistemological Beliefs and Metacognitive Strategies in Cuban University Students

MaybÍ Morell<sup>a1</sup>

<sup>1</sup>Independent Scholar

*The epistemological beliefs and metacognitive strategies of a sample of university students of Electric Engineering are discussed in this short overview. Significant differences between promoting and non-promoting groups were found regarding both beliefs and strategies. A strong correlation effect was also found between the strategies and beliefs about the structure of knowledge and the ability to learn.*

## Introduction

Since 1990, the study of the personal epistemology adopted a multidimensional perspective when it was introduced the idea of a system of epistemological beliefs (EB), or beliefs about the nature of knowledge and learning (Schommer, 1990). Personal epistemology was conceived as a system of multiple, more or less independent beliefs: a) the stability of knowledge, ranging from tentative to unchanging; b) the structure of knowledge, ranging from isolated bits to integrated concepts; c) the source of knowledge, ranging from handed down by authority to gleaned from observation and reason; d) the speed of learning, ranging from quick learning to gradual; and e) the control of learning, ranging from fixed at birth to live-long improvable.

Nowadays, these EB are known to play an important role in learning (Hofer and Pintrich, 1997; Schommer-Aikins, 2004; Metallidou, 2013; Sajovi et al, 2013). Several studies support that EB can predict the academic performance. In Cuba, studies have targeted the connection of personal epistemology to performance in specialized domains like Physics (Morell and Manzano, 2010) and Mathematics (VizcaÍno et al, 2015).

Metacognitive strategies (ME) are referred to those actions the subject performs before, during and after the learning process in order to optimize the execution of specific learning tasks. In general, the effect of the ME in learning seems to be significant, even though the reports can be controversial (Mason, 1994; Zusho and Pintrich, 2003)

In Morell and Manzano, 2019, the hypotheses of the study are: (H1) The EB differs between promoting and non-promoting groups of Engineering students; (H2) The use of ME differs between promoting and non-promoting groups; (H3) There are meaningful relations between EB and ME.

## Participants

This study included 119 first-year junior students, about 70% of the total first year students, from the specialty of Electric Engineering at the Technical University of Havana (CUJAE). Age range was 18-22 years ( $M = 19.6$ ;  $St. Dev. = 1.01$ ). Boys accounted for 77.3% of the sample, and girls for 22.7%. All classrooms were approximately equally represented.

## Materials and Procedure

EB were measured using the Epistemological Questionnaire (EQ) designed by (Schommer, 1990) and the ME the State Metacognitive Inventory (SMI) (O'Neil and Abedi, 1996). The individual academic achievement was acquired by collection of scores, identifying the students who passed to the next academic year (promoting group) and those who didn't (non-promoting group). The fractions were respectively 61% and 39% of the sample. For students in the promoting group a Great Point Average (GPA) was also calculated. The identified pending subgroup, within the promoting group, was about 28% of the total sample.

## Results

### EB and ME in promoting and non-promoting groups

Through factor analysis, using the 12 subsets established in the EQ, a factorial structure was generated for the EB. These are: Speed of Knowledge (naive form: Quick Learning), Structure of Knowledge (naive form: Simple Knowledge), Learning Ability (naive form: Fixed Ability) and Source of Knowledge (naive form: Knowledge handed down by Authority).

We evaluated the contrast between students in promoting and not-promoting groups, regarding the EB. The belief in the structure of knowledge is more sophisticated in promoting students than in the non-promoting group ( $t = 2.15$ ,  $p < .03$ ). That is, students that did not pass to the next year believes more in simple knowledge, while students that passed believe more that knowledge is rather complex.

We also looked at Pearson correlations between GPA and the EB in the promoting group. These results are shown in Table 1. A significant correlation appears in the belief on the source of knowledge. In this way, the less the students believe in knowledge as handed down by authority, the better GPA they earned.

Contrasts between the groups were also encountered regarding the ME. It was found that the employment of self-checking is significantly higher in the promoting group compared to the not-promoting ( $t = 3.02$ ,  $p < .003$ ). Moreover, the results show significant difference regarding the employment of self-checking within the promoting group, i.e. between pending and non-pending ( $t = 2.61$ ,  $p < .01$ ). For these two sub-

	QL	SK	FA	KHA
GPA	$r=-0.09$ $p=0.523$	$r=-0.13$ $p=0.357$	$r=0.12$ $p=0.400$	$r=-0.38^{**}$ $p=0.006$

Table 1: Pearson coefficient  $r$  and its significance  $p$  between the GPA and belief dimensions. QL: Quick Learning; SK: Simple Knowledge; FA: Fixed Ability; KHA: Knowledge handed down by Authority.

groups, planning employment also leads to a significant contrast ( $t = 2.32, p < .03$ ). That is, students promoting with pending matters uses planning and self-checking significantly less than promoting students without pending matters.

#### Particular relations between ME and EB

A correlation analysis was conducted relating the belief dimensions to the strategy categories, finding a number of significant Pearson values. Results are shown in Table 2. As can be seen, the less the students believe in simple knowledge, the more self-checking, planning and awareness they use in their metacognitive activity. Furthermore, the less the students believe in fixed ability to learn, the more self-checking and cognitive strategies they display.

	QL	SK	FA	KHA
S	+0.03	-0.53*	-0.32*	+0.10
CS	+0.07	-0.04	-0.23*	+0.12
P	-0.19	-0.35*	-0.09	-0.03
A	-0.08	-0.32*	-0.07	-0.02

Table 2: Pearson coefficients of correlation analysis between categories of metacognitive strategies and dimensions of epistemological beliefs. S: Self-checking; CS: Cognitive Strategy; P: Planning; A: Awareness. \*  $p < 0.05$ .

#### Conclusions

Metacognition and personal epistemology were studied through quantitative variables, as well as their relation with the academic achievement, in a sample of Engineering students from a typical low-achievement context. The EB showed a four-factors structure. Significant correlations were encountered between the beliefs in structure and source of knowledge and the strategies of planning and self-checking. In turn, all the four constructs were shown to be significantly connected to the academic achievement. In summary, a better academic performance was linked to better employment of planning and self-checking strategies, as well as to the belief in knowledge as a complex process, derived from reason rather than authority. This study contributes to frame a low-achievement scenario within a learning model centered in the subject, where students' beliefs and self-monitoring abilities play an essential role.

#### Notes

a. Email: maybimorell@gmail.com

#### References

- Hofer, B. K. & Pintrich, P. (1997). The development of epistemological theories: beliefs about knowledge and knowing and their relation to learning. *Review of Educational Research* 67, 68
- Mason, L. (1994). Cognitive and metacognitive aspects in conceptual change by analogy. *Instructional Science* 22, 157-187
- Metallidou, P. (2013). Epistemological beliefs as predictors of self-regulated learning strategies in middle school students. *School Psychology International* 34, 283-298
- Morell, M. & Manzano, M. (2010). Creencias epistemológicas y rendimiento académico en estudiantes de ingeniería. In *Memorias del Taller de Enseñanza de la Física*. 15 Convención Científica de Ingeniería y Arquitectura, La Habana, Cuba
- Morell, M. & Manzano, M. (2019). Are Low-Achievement Classrooms Cognitively Unbalanced? *International Journal of Education and Psychological Research* 8(1), 20-26
- O'Neil, H. & Abedi, J. (1996). *Reliability and validity of a state metacognitive inventory: Potential for alternative assessment (Tech. Rep.)* University of South California
- Savoji, A. P., Niusha, B. & Boreiric L. (2013). Relationship Between Epistemological Beliefs, Selfregulated Learning Strategies and Academic Achievement. *Procedia - Social and Behavioral Sciences* 84, 1160-1165
- Schommer, M. (1990). Effects of beliefs about the nature of knowledge on comprehension. *Journal of Educational Psychology* 82, 498-504
- Schommer-Aikins, M. (2004). Explaining the epistemological belief system: Introducing the embedded systemic model and coordinated research approach. *Educational Psychologist* 39, 19-2
- Vizcaíno, A., Manzano, M. & Casas, G. (2015). Validez de Constructo y Confiabilidad del Cuestionario de Creencias Epistemológicas sobre la Matemática en Alumnos de Secundaria Básica. *Revista Colombiana de Psicología* 24 (2), 301-316
- Zusho, A. & Pintrich, P. (2003). Skill and hill: The role of motivation and cognition in the learning of college chemistry. *International Journal of Science Education* 25(9), 1081-1094

# An Entropic-Energetic View for the Dynamics of HIV Infection

Ramon E. R. Gonzalez<sup>a1</sup>

<sup>1</sup>Laboratorio de Sistemas Complexos e Universalidades. Departamento de Física, Universidade Federal Rural de Pernambuco, 52171-900, Recife, Pernambuco, Brazil

*We propose a time-based analogy between the thermodynamic behavior of a three-level energy system and the progression of HIV infection described by the evolution of the cell population.<sup>b</sup>*

The CA model proposed by R.M. Zorzenon dos Santos et al. [1] is re-examined, from the perspective of the thermodynamic behavior of a three-level energy system. The evolution of the infection happens in the model based on well-defined rules. Therefore, figure 1 shows a simulation of the dynamics of the HIV infection generated from the CA model proposed by the authors, after the occurrence of the primary infection stage. In this model, we assume that each stage of the automata evolution (one week) the macroscopic states are in thermodynamic equilibrium with well-defined energy and entropy. All according to the average populations of CD4+T Cells, defined as healthy, infected and dead states from the CA model. We designed a three-level physical model to describe the dynamics of HIV infection (without treatment), analogous to that proposed as reported in the literature [2], considering the CD4+T cell population is characterized by its three possible states: infected  $N_1(t)$ , healthy  $N_2(t)$  and dead  $N_3(t)$ . Figure 2 illustrates the energy and transition diagram of the proposed model. The relative values between these energies are fixed from the populations of each state at the threshold of the onset of AIDS, that is, when  $n_1^* \sim 0.7$ ,  $n_2^* \sim 0.2$  and  $n_3^* \sim 0.1$ , respectively, where  $n_i = N_i/N$ , ( $i = 1, 2$ , and  $3$ ).

In terms of the variables of the HIV infection model, one can write the following equations:

$$n_1(t) + n_2(t) + n_3(t) = 1 \quad (1)$$

$$\mathcal{E}_1 n_1(t) + \mathcal{E}_2 n_2(t) + \mathcal{E}_3 n_3(t) = \mathcal{E}(t) \quad (2)$$

$$\mathcal{S}(t) = - \sum_{i=1}^3 n_i(t) \log n_i(t) \quad (3)$$

In the equations above  $\mathcal{E}(t)$  and  $\mathcal{S}(t)$  label the energy (in units of  $k_B T$ ) and the entropy (in units of  $k_B$ ) per particle at the instant  $t$ , respectively.

In our correspondence between the CA model and the 3-level energy model, the transition probabilities  $P_{D \rightarrow H}$  and  $P_{D \rightarrow I}$ , which represent the reposition of dead cells, are mimicked in the 3-level model by the respective Boltzmann weights, as indicated in the equations:

$$P_{D \rightarrow H} = p_r(1 - p_i) \propto e^{-(\mathcal{E}_2 - \mathcal{E}_3)} \quad (4)$$

$$P_{D \rightarrow I} = p_r p_i \propto e^{-(\mathcal{E}_1 - \mathcal{E}_3)} \quad (5)$$

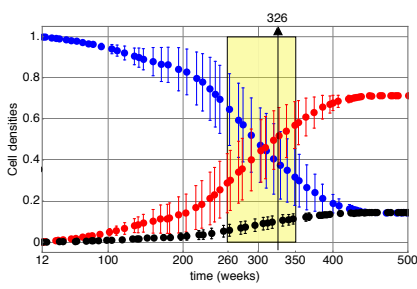
As it can be seen in Figure 2, the direct transition from the infected to the healthy state is absent once this process is prohibited by any mechanism.

In Figure 3, the region of the spectrum with negative energies  $\mathcal{E} \sim -1.8$  corresponds to states in which the population of infected cells not yet exceeds that of uninfected cells (healthy + dead), which occurs on average until week 320 after the peak of primary infection. Up to  $\mathcal{E} \sim -5.4$ , we observed a deterioration in the probability density function  $P(\mathcal{E})$ . This global behavior shows the highest occupancy in the most negative energy levels, due to the predominance of healthy cells at this stage. In the dynamics of infection, this occurs during the clinical latency period of up to  $\sim 231$  weeks (average). The peak observed around  $\mathcal{E} \sim 6.5$  corresponds to the dynamics of the infection in the time interval between 165 and 188 weeks, where the probability of the appearance of compact structures becomes significant [3], which leads the course of the infection to the inexorable beginning of AIDS. Positive energy values indicate the predominance of infected cells (high energies) when the unwanted development of AIDS is established with the collapse of the immune response from week  $\sim 350$  (average).

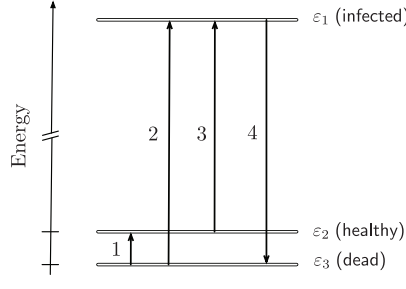
In Figure 4: (i)  $10 < t < 200$  weeks corresponding to the clinical latency period, the density of infected cells is low and increases linearly with time; (ii)  $200 < t < 450$  weeks corresponding to the onset of AIDS, which is the density of infected cells when the growth rate of them approximately doubles and finally; (iii)  $t \geq 450$  weeks, when the infected cell rate reaches its maximum value and becomes stationary. Figure 5 shows the behavior of the entropy of the system as a function of time.

The growth decreases continuously to zero in Figure 4, characterising the instant where the temperature signal change occurs. Subsequently, the entropy in Figure 5 decreases steadily until reaching the steady-state equilibrium value (full establishment of AIDS). The instant the entropy reaches its maximum value marks the change from the regime of positive to negative temperatures as indicated in Figure 3. This value corresponds to negative but close-to-zero energy values. Analysing dynamics of HIV infection (no treatment), we conclude that the dominant state of infected cells is the one where the highest energy level is *populated* with the majority of cells characterizing by negative values of absolute temperature. In these circumstances, the infected state becomes the state of equilibrium of the system.

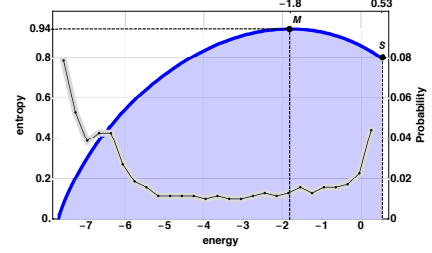
From the temporal evolution of the entropy, we ob-



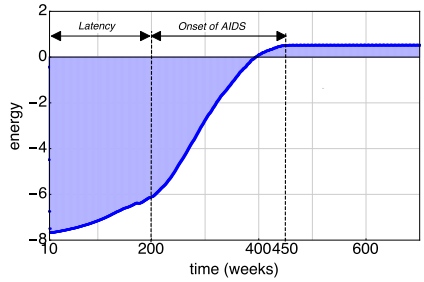
(1) Fractions of CD4 T+ cells healthy (blue), infected (A and B) (red) and dead (black) as a function of time (weeks).



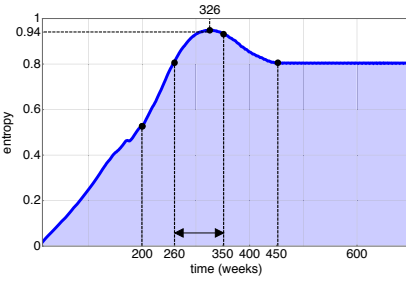
(2) Scheme of the energy levels and the transitions between the states of the three cell populations prescribed by the model: E1 for infected, E2 for healthy and E3 for dead cells respectively. The arrows indicate the direction of possible transitions.



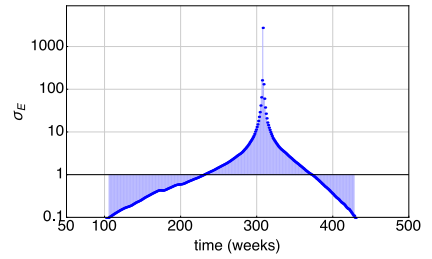
(3) Histogram of the energy distribution (right y-axis)  $P(\mathcal{E})$  for energy states with positive ( $\mathcal{E} < -1.8$ ) and negative temperatures ( $\mathcal{E} > -1.8$ ), and time-dependent parametric behavior of entropy as a function of energy (left y-axis).



(4) Energy evolution from 10 to ~200 weeks: clinical latency phase. From ~200 to ~450 weeks: development of AIDS.



(5) Entropy evolution (weeks). Interval (260 – 350) weeks is the time lag for occurrence of high fluctuations on cell concentrations.



(6) Semi-log plot of Energy relative error dynamics, same parameters used in Figure 1

served a linear monotonic growth until approximately  $t \sim 200$  weeks, when the appearance of partially ordered and compact spatial structures occurs with predominance of sequestering cells over the number of infected cells. With the growth of entropy in the first half of clinical latency, the system information losses are associated with the dynamic correlation losses that happen in  $t \simeq 200$  weeks. This loss of correlation can be tracked through the statistical behavior of the dynamics of infection via random matrix (RM) theory [3].

We found in Figure 5 that there is a small region of energy fluctuations with still negative values but corresponding to negative temperatures. In the dynamics of infection, this region corresponds to the time interval between  $\sim 260$  and  $\sim 326$  weeks, when the “crossing” of the densities of infected and uninfected cells occurs, as mentioned above. To quantify the energy fluctuations and to establish a criterion specifying the region where absolute inversion occurs between infected and uninfected cell populations, we define the relative deviation  $\sigma_{\mathcal{E}}$  as the ratio between the mean square deviation of the energy,  $\delta\mathcal{E}$ , and its absolute value:

$$\sigma_{\mathcal{E}} = \frac{\delta\mathcal{E}}{|\mathcal{E}|}. \quad (6)$$

In Figure 6, fluctuations of order  $10^3$  higher than the

absolute value of the energy are responsible for the states in which energy and temperature are both negative. The instants for which  $\sigma_{\mathcal{E}} = 1$  correspond to  $t = 231$  and  $t = 372$  weeks, the beginning and end of the transition, respectively. These values fit the region where the error bars overlap, as shown in Figure 1.

**Notes**

- a. Email: ramayo\_g@yahoo.com.br
- b. Original version of this article is Ref. [4]

**References**

[1] Rita Maria Zorzenon dos Santos and Sérgio Coutinho, *Physical Review Letters*, **87** (2001) 168102

[2] Daan Frenkel and Patrick B. Warren, *Am. J. Phys.*, **83** (2015) 163

[3] Ramón E. R. González, Iury A. X. Santos, Marcos G. P. Nunes, Viviane M. de Oliveira and Anderson L. R. Barbosa, *Physics Letters A*, **381** (2017) 2912-2916

[4] Ramón E. R. González, P. H. Figueirêdo, S. Coutinho, *Physica A: Statistical Mechanics and its Applications* (2020) in press

# Degradation of two chlorinated pesticides using advanced oxidation processes

Germán Cruz González<sup>1,2</sup>, Carine Julcour<sup>1</sup>, Sarra Gaspard<sup>3</sup>, and Ulises Jáuregui Haza<sup>a4</sup>

<sup>1</sup>Laboratoire de Génie Chimique, Université de Toulouse, Toulouse, France

<sup>2</sup>Instituto Superior de Tecnologías y Ciencias Aplicadas (InSTEC), UH, Habana, Cuba

<sup>3</sup>Laboratoire COVACHIM M2E, Université des Antilles, Pointe à Pitre, Guadeloupe

<sup>4</sup>Instituto Tecnológico de Santo Domingo (INTEC), República Dominicana

*The degradation of chlordecone and beta-hexachlorocyclohexane in aqueous media is possible by means of photolysis, (photo-)Fenton oxidation and ozonation processes.*

Banana and sugarcane have been the main agricultural products of the French Antilles (Guadeloupe and Martinique) since the 1960s. To prevent crop damage from the banana weevil, chlorinated pesticides, such as chlordecone (CLD,  $C_{10}Cl_{10}O$ , CAS-number: 143-50-0),  $\beta$ -hexachlorocyclohexane ( $\beta$ -HCH,  $C_6Cl_6H_6$ , (CAS-number: 319-85-7) and dieldrine were extensively used until the beginning of the 1990s, resulting in the contamination of both the soil and the surface waters [1]. It was not until 2009, when they were listed as persistent organic pollutants under the Stockholm Convention, that the production and agricultural use of the first two pesticides was prohibited worldwide.

Thus, there is growing need to find remediation solutions for CLD and  $\beta$ -HCH problem. The advanced oxidation processes (AOP) like (photo-)Fenton oxidation or ozonation have been applied for the degradation of several classes of pesticides and refractory compounds. This work examines the degradation of CLD and  $\beta$ -HCH in synthetic aqueous solutions by means of photolysis, (photo-)Fenton oxidation and ozonation [2].

## Comparison of the different AOPs for CLD degradation

Photolysis, (photo-)Fenton oxidation and ozonation were investigated for the removal of CLD (Fig. 1). It should be noticed that although hydroxyl radicals generated by AOP are reported to be highly reactive and non-selective, Fenton oxidation did not yield any significant conversion of the contaminant in the investigated condition. On the other hand, ozone was able to achieve 70% of pesticide removal within 2 hours. In this case, both molecular and radical mechanisms should be involved, the latter being favoured by high pH values [3]. An inhibition of radical process could be then suspected.

CLD could be readily degraded by direct photolysis, to more than 95% in 3 hours. Addition of the Fenton's reagent resulted in no appreciable improvement of the removal rate, and thus hydroxyl radical mechanism that should be enhanced under UV-Vis irradiation did not seem to play any noticeable role either.

To further investigate photo-assisted processes, the

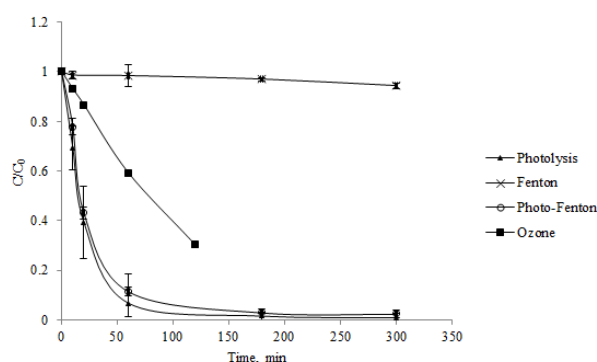


Figure 1: Degradation of CLD by photolysis, Fenton, photo-Fenton and ozonation processes.  $[CLD]_0 = 2 \mu\text{mol.L}^{-1}$ ,  $T = 30^\circ\text{C}$ ; 450 W MP Hg lamp and quartz lamp holder for photo-assisted processes;  $[H_2O_2]_0 = 0.6 \text{ mmol.L}^{-1}$ ,  $[Fe(II)]_0 = 0.3 \text{ mmol.L}^{-1}$  and  $\text{pH}_0 = 2.6$  for Fenton-based oxidation.

applied wavelength range was varied by using the MP Hg lamp with a glass immersion well and a LP Hg lamp with quartz lamp holder (Fig. 2).

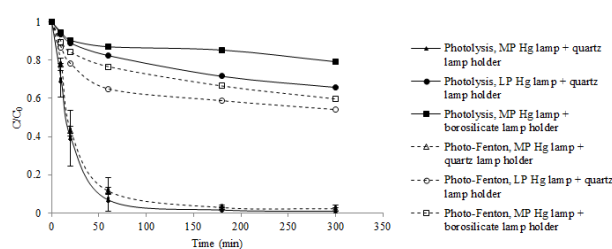


Figure 2: Effect of irradiation spectrum on the degradation of CLD by photo-assisted processes.  $[CLD]_0 = 2 \mu\text{mol.L}^{-1}$ ,  $T = 30^\circ\text{C}$ ; photo-Fenton:  $[H_2O_2]_0 = 0.6 \text{ mmol.L}^{-1}$ ,  $[Fe(II)]_0 = 0.3 \text{ mmol.L}^{-1}$ ,  $\text{pH}_0 = 2.6$ .

For both the processes, the removal yield of CLD ranged in the order: MP Hg lamp + quartz lamp holder > LP Hg lamp + quartz lamp holder > MP Hg lamp + borosilicate lamp holder. As photolysis mechanism was shown as the dominant process, this could be explained by the absorbance spectrum of the molecule which exhibited maxima at 210 and 320 nm and differences in lamp irradiation intensity in this wavelength

range. Cutting (first) absorption maximum of CLD at 210 nm strongly reduced the molecule photodegradation. On the other hand, the higher rate observed at  $\lambda = 254$  nm than at  $\lambda > 280$  nm (while another absorption peak is observed at 320 nm) might be due to the presence of acetone, which was reported to act as photo-sensitizer [4]. Moreover, when the glass lamp holder dramatically hindered photolysis, effect of Fenton's reagent addition more clearly stood out, indicating that a radical-mediated mechanism in fact contributed, but to a much lower extent.

### Comparison of the different AOPs for $\beta$ -HCH degradation

The results of  $\beta$ -HCH degradation by AOP exhibit essentially the same features than for CLD: almost insignificant oxidation rate by Fenton's reagent and thus a photo-Fenton process mainly driven by the direct photolysis of the molecule.

Effect of lamp irradiation was also investigated (Fig. 3) and the most striking result was a still high elimination of  $\beta$ -HCH by photo-Fenton oxidation under UVB-Vis. Only scarce information related to the advanced oxidation of this pesticide has been reported. Ormad et al. [5] studied the degradation of a group of pesticides including  $\beta$ -HCH in very diluted conditions ( $0.5 \mu\text{g}\cdot\text{L}^{-1}$ ) by ozonation,  $\text{O}_3/\text{H}_2\text{O}_2$ ,  $\text{O}_3/\text{TiO}_2$  and  $\text{O}_3/\text{H}_2\text{O}_2/\text{TiO}_2$  processes. Only  $\text{O}_3/\text{H}_2\text{O}_2/\text{TiO}_2$  treatment was able to degrade  $\beta$ -HCH and yielded 10% conversion of the molecule with  $3 \text{ mg}\cdot\text{L}^{-1}$  of ozone dosage, so a ratio of  $\text{O}_3/\text{pollutant}$  close to the one applied here ( $6 \text{ g}/\text{mg}$  vs.  $8.6 \text{ g}/\text{mg}$  in the present study).

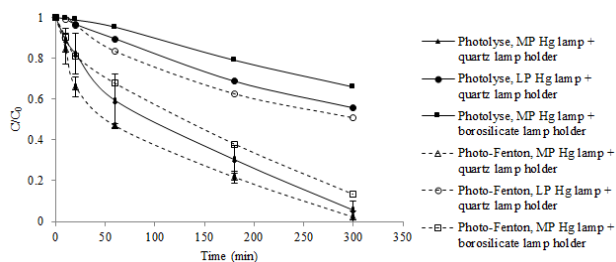


Figure 3: Effect of irradiation spectrum on the degradation of  $\beta$ -HCH by photo-assisted processes.  $[\beta\text{-HCH}]_0 = 3.4 \mu\text{mol}\cdot\text{L}^{-1}$ ,  $T = 30^\circ\text{C}$ ; photo-Fenton:  $[\text{H}_2\text{O}_2]_0 = 0.8 \text{ mmol}\cdot\text{L}^{-1}$ ,  $[\text{Fe(II)}]_0 = 0.4 \text{ mmol}\cdot\text{L}^{-1}$ ,  $\text{pH}_0 = 2.6$ .

Preliminary identification of degradation products indicated that hydrochlordecone was formed during photo-Fenton oxidation of CLD, while for  $\beta$ -HCH the major product peak exhibited  $\text{C}_3\text{H}_3\text{Cl}_2$  as most abundant fragment.

In order to compare the different processes studied for the degradation of both pesticides, their kinetics constants were calculated following a pseudo-first order model. The results show that for the CLD the best process was the photolysis, followed by the photo-Fenton and the ozone, all with the same order of magnitude, and the Fenton process was the less effective with 2 orders of magnitude below. In the case of  $\beta$ -HCH, the behavior was similar to CLD but the photolysis and photo-Fenton processes has the same rate constants.

On the other hand,  $\beta$ -HCH was found less sensitive to UV irradiation, its first-order photolysis rate constant being  $2.10^{-4} \text{ s}^{-1}$ , much smaller than that of CLD ( $8.10^{-4} \text{ s}^{-1}$ ).  $\beta$ -HCH also showed a slightly lower reactivity towards ozone, with about 50% conversion after 2 hours (against 70% for CLD).

### Summarizing

In the investigated conditions, both chlordecone and beta-hexachlorocyclohexane exhibited a much lower reactivity towards Fenton's reagent ( $< 10\%$  conversion in 2 hours) than ozone ( $> 50\%$  conversion). Photolysis achieved almost complete removal of both pesticides within 5 hours when using a high pressure mercury lamp, and a conversion of about 40% with a low power lamp at 254 nm. Preliminary identification of degradation products indicated that hydrochlordecone was formed during photo-Fenton oxidation of CLD, while for  $\beta$ -HCH the major product peak exhibited  $\text{C}_3\text{H}_3\text{Cl}_2$  as most abundant fragment.

### Notes

a. Email: ulises.jauregui@intec.edu.do

### References

- [1] Y.M. Cabidoche, R. Achard, P. Cattan, C. Clermont-Dauphin, F. Massat, J. Sansoulet., *Environmental Pollution*, **157** (2009) 1697-1705
- [2] G. Cruz-González, C. Julcour, H. Chaumat, S. Gaspard, U. Jáuregui-Haza., *Journal of Environmental Science and Health, Part B*, **53** 2 (2018) 121-125
- [3] GA. López-López, J.S. Pic, H. Debellefontaine, *Chemosphere*, **66** (2007) 2120-2126
- [4] W. Chu, S.M. Tsui, *Chemosphere* **39** (1999) 1667-1677
- [5] M.P. Ormad, N. Miguel, M. Lanao, R. Mosteo, J.L. Ovelleiro., *Ozone-Science and Engineering* **32** (2010) 25-32

# Evaluation of the Molecular Inclusion Process of Organochlorine Pesticides at Cyclodextrins

Anthuan Ferino-Pérez<sup>a1</sup>, Juan José Gamboa-Carballo<sup>1,2</sup>, and Ulises Jáuregui Haza<sup>3</sup>

<sup>1</sup>Instituto Superior de Tecnologías y Ciencias Aplicadas (InSTEC), Universidad de La Habana, Cuba

<sup>2</sup>Department of Chemistry and Applied Biosciences, ETH Zürich, Switzerland

<sup>3</sup>Instituto Tecnológico de Santo Domingo (INTEC), República Dominicana

*The molecular inclusion process of two organochlorine pesticides and its radiolabeled analogous with cyclodextrins is a perspective technology for the removal of these pollutants from water.<sup>b</sup>*

Persistent organic pollutants (POPs) are those substances that, in addition to their toxicity, present an elevated residence time in the environment due, principally, to a high chemical or biological resistance to degradation and to the fact that they were poured to nature in quantities that overcome the capacity of the natural media to degrade them. Specifically organochlorine pesticides such as chlordecone (CLD, C<sub>10</sub>Cl<sub>10</sub>O, CAS: 143-50-5) and  $\beta$ -hexachlorocyclohexane ( $\beta$ -HCH, C<sub>6</sub>H<sub>6</sub>Cl<sub>6</sub>, CAS: 319-85-7) are of great concern because they were profusely used around the world, they have an extremely high environmental stability and cause severe affectations to human, animals, and environmental health. Due to these facts, they were included since 2009 in the list of POPs by Stockholm's Convention.

In the last years, the search for strategies for water decontamination centered on organochlorine pesticides removal was prompted. The decontamination methods used range from advanced oxidation process and biodegradation treatments, to the use of activated carbon for the treatment of polluted water by adsorption. In spite of these efforts, it is still necessary to increase the efficiency of the separation methods used, which has promoted the search for new alternatives, like the formation of host-guest complexes with cyclodextrins (CDs) [1].

The mathematical modeling of the interactions pollutant/decontaminant-agents through the application of computational chemistry methods allow saving material resources while optimizing the time and security of the researchers. Particularly, the molecular inclusion complexes formed between the CDs and different molecules have been studied by several computational methods. However, in previous works, the authors directly set the molecule of interest in contact with the interior of the CD cavity in certain configurations based, largely, on chemical intuition. Also, generally, only the  $\beta$ -CD is considered as a host molecule, ignoring the possibility of better encapsulation capacities of other CDs, especially the  $\gamma$ -CD. In our works, a more general approach was used, based on the random exploration of the configurational space of the host-

guest complexes of pesticides at each of the three natural occurring CDs ( $\alpha$ -,  $\beta$ -, and  $\gamma$ -CD).

## Nanoaggregates of CLD and $\beta$ -HCH with CDs

In order to correctly evaluate the chemical behavior of CDs a theoretical study of their conformational equilibria was performed by Gamboa-Carballo et al [2]. Eight symmetrical conformers, which differ in their intermolecular H-bond patterns were found and characterized for each CD. The results obtained are in agreement with X-ray diffraction data helping to validate the results of this work. These calculations showed that four of the eight studied conformers for each CD are the most populated in aqueous solution. The eight conformers are showed in Figure 1.

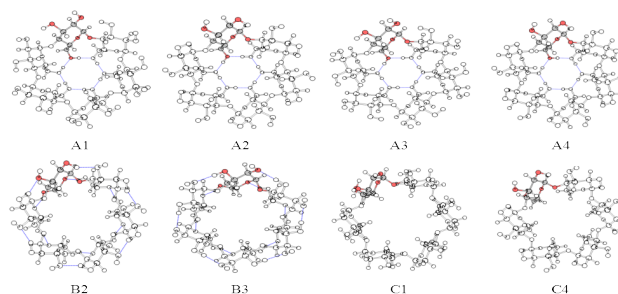


Figure 1: CDs' symmetrical conformers. Only the  $\alpha$ -CD is presented and a glucopyranose unit is highlighted in each conformer.

Multiple Minima Hypersurface methodology, which combine a semiempirical Hamiltonian with statistical thermodynamic calculations, was employed for performing a thorough exploration of the configuration space of the nanoaggregates and evaluating the association thermodynamic properties that describe the molecular inclusion process. Figures 2a and 2b show the mean association energy for the complexes CLD@CDs [3] and  $\beta$ -HCH@CDs [4] respectively.

As could be seen, there is a remarkable stabilization of the systems when  $\gamma$ -CD is the host molecule for all evaluated conformers. In both cases, there is a progressive stabilization of nanoaggregates as the size of the CDs cavity increase for the conformers B2, B3,

C1, and C4. Of these conformers, representative structures of inclusion complexes were selected for posterior refinement. In all the cases, the global minima and additional structures of interest for the presented geometry were selected. This selection was made always taking into account that these structures had a population greater than 10% according to a Boltzmann distribution.

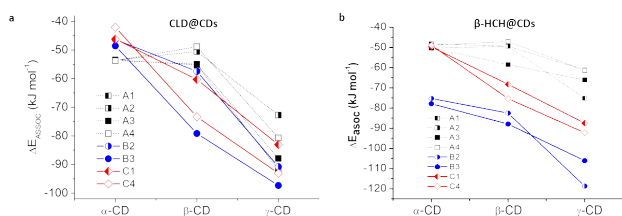


Figure 2: Mean association energies (calculated by MMH methodology) of (a) CLD and (b)  $\beta$ -HCH with the conformers of studied CDs.

The refinement of complexes geometries, association energies, and wavefunctions was performed through DFT calculations using the meta-GGA hybrid functional M06-2X with the Pople's basis 6-31G(d,p). SMD was employed as implicit solvent model and Grimmer dispersive corrections were applied for all calculations. The association energy here calculated was corrected for mitigating Basis Set Superposition Error (BSSE) with a method developed by the authors [3]. These calculations confirmed that the more stable complexes are formed when  $\gamma$ -CD is the host molecule. The conformers B3 and C1 are the more stable ones for both pesticides.

For characterizing the interactions present in these complexes Quantum Theory of Atom in Molecules was applied using the Nakanishi criteria for determinate the type of the interactions from density dependent functions. With this analysis we concluded that the great number of dispersive interactions (with a minimum of 17 interactions between the pollutant and the CD) together with the presence of other interactions of greater strength as H-bonds, dihydrogen bonds, and halogen bonds contribute to explain the stability of this complexes in spite of the absence of covalent interactions. Theoretical results for CLD@CDs system are in agreement with the experimental results obtained in 2016 by Rana et al. [1], while the ones of  $\beta$ -HCH@CDs complexes were confirmed through spectroscopic measurements and microscopy analysis performed by Ferino-Pérez et al. [4].

### Radiolabeled analogous as radiotracers of the system

The determination of CLD and HCH in water represents a challenge for the analytical chemistry due to pesticides low concentrations in nature that in occasions are found below the quantification limit of many modern analytical methods. The labeling with a radioactive isotope might be an effective approach for

studying their distribution in nature and its biodistribution in several living organisms, as well as for evaluating several remediation technologies for the CLD and the  $\beta$ -HCH in their typical concentrations' conditions. However, for a compound would be a suitable radio-tracer it should resemble the behavior of its analogous inside the study system.

The work of Jáuregui-Haza et al [5] theoretically evaluated the feasibility of using radio-iodine labelled analogous of these pollutants as radiotracers of the systems under study. Results obtained in this investigation allow us to verify this hypothesis. Figure 3 shows the similarity that exists in the geometries and interactions present when compared the complexes formed with the pesticide with the ones of their iodine analogous.

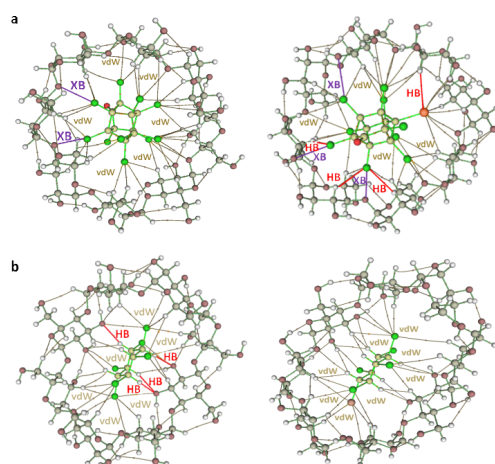


Figure 3: Intermolecular interactions of molecular inclusion complexes (a) CLD@C1- $\gamma$ -CD and I-CLD@C1- $\gamma$ -CD and (b)  $\beta$ -HCH@C1- $\gamma$ -CD and I- $\beta$ -HCH@C1- $\gamma$ -CD determined by QTAIM analysis. The different types of interactions are identified as: dispersive (vdW, in yellow), hydrogen bond (HB, in red) and halogen bond (XB, in purple).

### Notes

a. Email: anthuanferp@gmail.com

b. Original version of this article is Ref. [4]

### References

- [1] Rana, V.K., Kissner, R., Gaspard, S., Levalois-Grütz-macher, J., *Chem. Eng. J.*, **293** (2016) 82-9
- [2] Gamboa-Carballo, J.J., Rana, V.K., Levalois-Grutz-macher, J., Gaspard, S., Jauregui-Haza, U.J., *Mol. Model.*, **318** (2017) 23
- [3] Gamboa-Carballo, J.J., Ferino-Pérez, A., Rana, V.K., Levalois-Grütz-macher, J.L., Gaspard, S., Montero-Cabrera, L.A., et al. J., *Chem. Inf. Model.*, (2020)
- [4] Ferino-Pérez, A., Gamboa-Carballo, J.J., Ranguin, R., Levalois-Grütz-macher, J., Bercion, Y., Gaspard, S., et al., *RSC Adv.*, **9** (2019) 27484-99
- [5] Jáuregui-Haza, U., Ferino-Pérez, A., Gamboa-Carballo, J.J., Gaspard, S., *Environmental Science Pollution Research*, (2020) 1-12

# Network of scientific collaboration of Cuban researchers working in Europe: Perspective for the home country

Miriam Palacios-Callender<sup>a1</sup>

<sup>1</sup>Faculty of Life Sciences and Medicine, King's College London, United Kingdom

*This study analyses the potential value of the network of scientific collaboration of Cuban researchers in Europe focussing on their institutional links with worldwide collaborators between 1995 and 2014.*

Countries investing in science to boost their economic growth are also engaging and supporting the international collaboration in science [1]. This exchange of knowledge generates borderless flows of researchers as actors of complex and global networks of scientific collaboration. The dilemma for developing countries is how to benefit from this global network of international collaboration without losing their best and brighter researchers. Premises for the right balance rest on strengthening the national capacity in science and optimising transnational knowledge practices of the mobile researchers to contribute to the national output in science from abroad and to build long lasting relationships for returning home [2].

Our research aimed to find the features of those premises in the case of Cuba. First, we investigated the Cuban scientific capacity [3]. Second, we focused on the performance of a sample of 107 Cuban researchers in Europe and their potential to bridge their network of collaboration from Europe with Cuban science [4]. Selecting the sample of researchers in this geographical region responds to the mobility trends during the period of study between 1995 and 2014 and the prospect of strengthening the scientific collaboration between Cuba and Europe. Another advantage of this region is the free movement of their researchers and the availability of flexible and inclusive funding in the European Research Area.

## Sample of Cuban researchers in Europe (CRiE)

We estimated by triangulation of three different sources that Cuban researchers in Europe might be between 600 to 1200 from the beginning to the end of the period of study. The ability to publish in scientific journals was the distinctive attribute to choose the sample. By publishing, scientists consider the knowledge as a public good, making possible a favourable environment for sharing information among collaborators. Figure 1 shows the experimental design followed in the process of finding the sample of the active Cuban researchers in Europe (CRiE). The initial list of researchers was created using the chain-referral sampling methodology, searching sources of professional network such as LinkedIn. The original number of candidates were 150 Cuban professionals in Europe. A further screening using the bibliographic database Scopus reduced the number to 135 Cuban researchers with at least one

record, of which 107 were included in the study as CRiE according to their publication pattern.

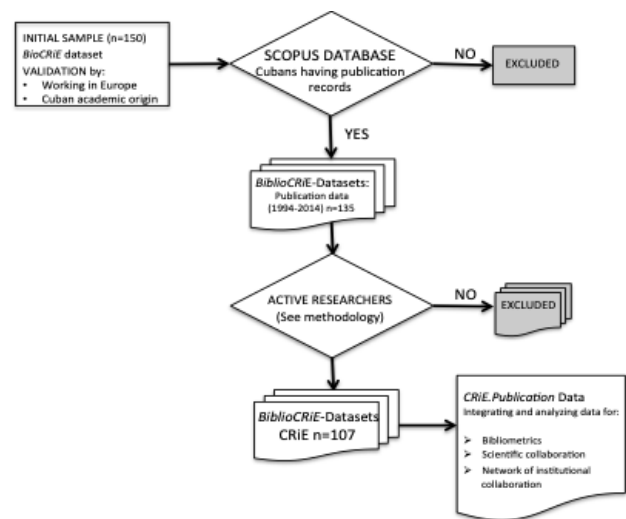


Figure 1: Experimental design. Source [4]

## Network of scientific collaboration of CRiE

The search in Scopus was carried out by using the Author search engine, limiting the number of documents to articles and fixing the period between 1995 and 2014. Publication records of each researcher with all available information was downloaded and codified anonymously creating 107 datasets (BiblioCRiEs). Another working dataset (Publication Data) integrating the bibliometric information was created in order to explore the institutional collaboration. By choosing institutions rather than countries we were able to assess the institutional actors (nodes) in the CRiE network of collaboration. Each publication with  $n$  collaborations generates  $n$  binary links of CRiE institutions (type I) with  $n$  collaborating institutions (type II). A third column (weight) counting the frequency of those binary ties between type I and type II institutions was also recorded (More explanation in [4], page 271, paragraph 3). The three columns of the binary relational matrix were then transformed in a symmetrical matrix using an ad hoc programme [5] and then processed through UCINET and NetDraw software for  $k$ -core analysis of centrality and the visualization of the institutional network of collaboration created by CRiE [6].

Institutions and links in CRiE network		
Sector	Institutions Nr(%)	Collaborations Nr(%)
Academia	14(40)	185(73.7)
Public Health	5(14.3)	8(3.2)
Industry	9(25.7)	39(15.5)
CITMA	7(20)	19(7.6)
Cuba/CRiE- Network	35/991	251/6842

Table 1: Cuban institutions in the network of CRiE

### Profile of CRiE and analysis of the network of scientific collaboration

CRiE have been publishing from 115 European institutions of which 80 were universities, 28 national or regional institutes of research and 7 institutions from the industry. CRiE accrued 2,385 scientific articles of which 1,863 were with European affiliation generating 1,348 collaborative articles between 1995 and 2014. The whole network of CRiE collaboration comprises 991 different institutions (nodes) from 56 countries: 698 from Europe, 118 from North America, 96 from Latin America and 79 from the rest of the world. European institutions sharing Latin roots are highly represented among institutions of the region in which Spain shares 24% of collaborative institutions, followed by Italy (15%) and France (14%).

The 1348 collaborative articles generated 3140 binary collaboration (ties) accruing 6842 frequencies of links. Fifty-six CRiE collaborated with Cuba producing 203 articles (203/1348, 15%) and 251 collaborative links (251/6842, 3.6%) with 35 Cuban institutions (Table 1). The majority of collaboration with Cuba took place during the first five years after moving to Europe.

$k$ -core analysis of centrality showed two Cuban universities sharing the central position ( $k = 6$ ) with another 24 institutions worldwide of which, 18 belong to academia. These Cuban institutions were the University of Havana and the Central University of Villa Clara. Another two and five Cuban institutions were in  $k$ -cores 4 and 3 respectively. The rest were in the periphery among 679 institutions (Figure 2).

### Summary

Building the network of international collaboration of CRiE by choosing the institutions as nodes, provides key information about where the Cuban actors of the network have been more successful. The network analysis of centrality informs which institutions are better connected and therefore benefited from the international collaboration in this particular network.

From Cuba's perspective it shows the positioning and the degree of penetration of Cuban institutions in the network of their mobile researchers, pointing where the country can build further cooperation and partnership. Cuban universities are the main actors in the Cuba-CRiE collaboration. More importantly,

this network of CRiE publishing with Cuban institu-

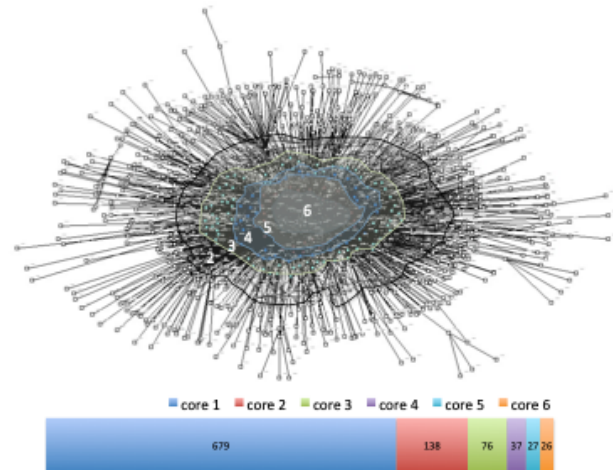


Figure 2: CRiE network of institutional collaboration. The horizontal bar shows number of institutions per core based on  $k$ -core analysis of centrality. Source [4]

tions helps to increase the visibility of Cuban scientific capacity, through international meetings and more diversified journals not always used by Cuban counterparts. This study shows that Cuban researchers naturally collaborate with the home country. There is scope for improvement addressing a long-term connection, and lessons to learn from the experiences of both sides: CRiE and the researchers from Cuban institutions. Monitoring the dynamic of the network can be a valuable tool to optimise the relationship between mobile researchers abroad and the national system of science and innovation, including their temporary or definitive return to work in Cuban institutions.

### Notes

a. Email: miriam.palacios-callender@kcl.ac.uk

### References

- [1] C. Franzoni, G. Scellato and P. Stephan, *Nature Biotechnology*, **30** 12 (2012) 1250-1253
- [2] K. Jonkers and R. Tijssen, *Scientometrics* **70** 2 (2008) 309-333
- [3] M. Palacios-Callender, R. A. Roberts and T. Roth-Berghofer, *Journal of Documentation* **72** 2 (2016) 362-390
- [4] M. Palacios-Callender and S.A. Roberts, *Scientometrics* **117** 2 (2018) 745-769
- [5] E. Marcet-Garcia, M. Palacios-Callender and M. Marcet, *Revista Hispánica para Análisis de Redes* **27** 1 (2016) 73-80
- [6] S.P. Borgatti, M.G. Everett and J.C. Johnson, *Analysing social networks*, London: Sage Publication Ltd (2013)

# MEMBIOSIM: a Submerged Membrane Bioreactor simulator for teaching its functioning

Yusmel González Hernández<sup>a1</sup>, Ulises Jáuregui Haza<sup>1,2</sup>, Claire Albasi<sup>3</sup>, and Marion Alliet<sup>3</sup>

<sup>1</sup>Instituto Superior de Tecnologías y Ciencias Aplicadas (InSTEC-UH), Universidad de La Habana, Cuba

<sup>2</sup>Instituto Tecnológico de Santo Domingo (INTEC), República Dominicana

<sup>3</sup>Laboratoire de Génie Chimique, Université de Toulouse, CNRS, INPT, UPS, Toulouse, France.

*The development of a submerged membrane bioreactor computer simulator that integrates biological degradation process with physical separation process is a useful tool for teaching and research.<sup>b</sup>*

The submerged membrane bioreactor (SMBR) technology has grown exponentially due to its advantages over conventional wastewater treatment processes, such as reduced environmental impact, improved effluent quality and better process control. The major potential advantage of this technology is found in the field of water reuse. Nevertheless, the effective application of membrane bioreactors (MBRs) is limited by membrane fouling and the associated cost and energy burdens [1]. At the same time, experimentation in these types of installations is very expensive and time consuming.

On the other hand, it is necessary to take all the elements mentioned above into account in the training of engineers and of the staff that will operate the SMBR. It is essential to develop tools, as simulators, that can help in the learning process, both at universities and at operator training centers. Another advantage of a simulator is its value in the training process from the research point of view: to help to solve problems that are as yet unsolved. Simulators are also an important support for the study of process optimization. The use of simulated experiments can considerably reduce the cost of a laboratory course, increase the number of experiments in the learning process and enable experiments to be carried out that would otherwise involve working with dangerous materials and/or in dangerous conditions [2]. The objective of this work is to develop a computer simulator of an SMBR and to show its potential in teaching how such processes work.

## Description and operation of the simulator

Description and operation of the simulator For teaching use, the SBRM computer simulator should be user friendly and provide an easily accessible introduction to the subject. Since other uses are advanced training and research, many parameters should be easily modifiable. The simulator shows a general standard scheme of the SMBR, which allows the main structural components of the system to be apprehended, so that the user can gain a better understanding of the installation performance and thus a better understanding of the processes that are involved in these types of in-

stallations [3]. The simulator allows the user to study the influence of 35 model input variables on 16 output parameters, which can be displayed graphically or numerically.

## Comparison of simulator performance with experimental data

To substantiate and justify the use of the computer simulator to study an SMBR, it is essential to know the level of approximation to which the mathematical model can reproduce SMBR operation. For this reason, the simulation results were compared with experimental data. The parameter chosen was the transmembrane pressure because of its importance in the operation of the SMBR [4, 5]. Figure 1 shows the experimental and calculated values of TMP.

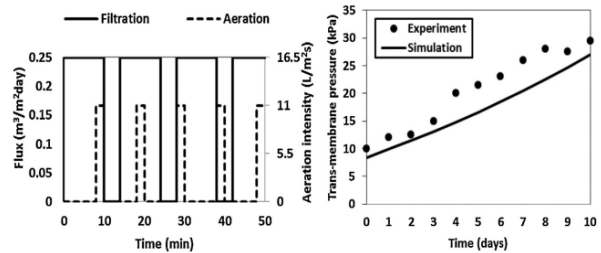


Figure 1: Comparison between the experimental data (points) and simulation results (line). The left-hand diagram shows the working conditions of the experiments.

A mean relative error of estimation of 15% was obtained. This result can be considered acceptable for predicting the behavior of a system of such complexity because, as explained above, the simulator was built by implementing a model that combines biological degradation with the filtration process. The biological system modelling introduces a high percentage of error as the input values of biological variables correspond to the mean values measured during the experiment [6]. Even with 15% of error, the simulator already gives the trends in the evolution of physical quantities and the order of magnitude of their values, which is the

information sought.

### Considerations about the practical activity

The practical activity [3]. was carried out successfully by the students. They showed their abilities in the use of computer programs and, in general, they managed the simulator with success. Nevertheless, there were some students who had difficulty solving this task because they did not understand the functioning of an SMBR correctly and others who had problems with the simulator language. However, with the instructor's help, they finished the proposed exercise correctly.

The students' correct use of the different simulator tools and their understanding of the SMBR operation was evaluated from their analysis of the results they reported.

The reports were corrected and graded according to the French norm, which gives points out of 20, with the following appreciation: 10 = pass, 12 = quite good, 14 = good, 16 = very good, 18 = excellent, and 20 = congratulations. The average was 13.6/20 with a minimum of 12/20 and a maximum of 16/20, which is a rather good result. Parts 1–4 were achieved very well, with only minor mistakes. Part 5 was completed in a more variable way, mainly due to a lack of time (and to the French way of teaching, which discriminates using time).

### Students' opinions

The students' responses to the questionnaire [3] are presented in Figure 2. A grading scale obtained by using numerical equivalents for the opinions: "Strongly agree" = 20, "Agree" = 13.33, "Disagree" = 6.67, "Strongly disagree" = 0 (in order to correspond to the French grading system, which is out of 20) has been added. For each of the statements proposed in the questionnaire, a "grade" is indicated, which was obtained by averaging the answers. To analyze these responses, the questions with the most numerous answers "Disagree" were considered as well as the ones with less good grades. The students' evaluations were very positive. This simulated laboratory aroused great interest in more than 95% of the students.

As noticed by the teaching staff during the practical activity, although some students had some difficulties in understanding the functioning of the simulator by themselves (Q4), the participation of the teacher helped them in this task (Q5).

Slightly more than 10% of the students did not agree that this laboratory was relevant to their program and the lowest evaluation concerned the situation of this laboratory in the education program (Q8). A discussion with the students showed that an additional experimental activity may help to improve this impression. The teaching staff is thinking about a convenient and not too expensive way to include it (visit to a water treatment plant, visit to a research experimental device, short experimental practical activity, etc.).

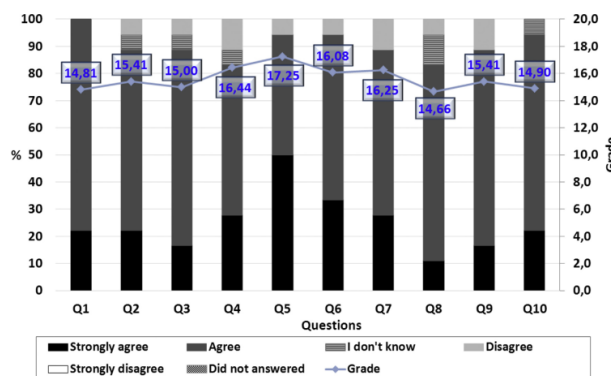


Figure 2: Results of the anonymous questionnaire.

### Summary

An SMBR computer simulator was built with recent modelling knowledge and a friendly interface. The results given by the simulator are accurate enough to provide the trends and orders of magnitudes of physical quantities needed for the teaching application of the simulated MBR. The practical use of the simulator was evaluated with the development of simulated laboratory work lasting three and a half hours, which gave results that would take more than fifteen months of real-world experiments. It was successfully applied and, achieved the most difficult objectives of enabling the students to analyze the influence of operating parameters on the SMBR functioning and being largely accepted by the students. While this has not been tested, it appears clear that the dynamic model used would permit the training of professionals.

### Notes

- Email: yusmel@instec.cu
- The original version of this article is Ref. [3]

### References

- [1] A. Menniti, E.J.W.R. Morgenroth., *Water Research*, **44** (2010) 5240-5251
- [2] E. Skorzinski, M. Shacham, N. Brauner. *In Computer Aided Chemical Engineering*, Elsevier (2009) 1233-1238.
- [3] Y. Hernández-Gonzalez, U. Jauregui-Haza, C. Albasi, M. Alliet., *Education for Chemical Engineers*, **9** (2) (2014) e32-e41.
- [4] F. Meng, et al., *Water Research*, **43** (2009) 1489-1512.
- [5] A. Fenu, et al., *Water Research*, **44** (2010) 4272-4294.
- [6] A. G. Zarragoitia, et al., *Journal of Membrane Science*, **325** (2008) 612-624.

# Novel HIV matrix shell structure and potential functions

Marcelo Marcet-Palacios<sup>a1,2</sup>

<sup>1</sup>Laboratory Research and Biotechnology, Northern Alberta Institute of Technology, Edmonton, Canada

<sup>2</sup>Alberta Respiratory Medicine, University of Alberta, Edmonton, Canada

*The structure of the HIV matrix shell has not been fully elucidated. In this article, I highlight contributions that led to a model composed of adjacent hexagons forming a sphere and mentioned studies that were subsequently impacted. A cross disciplinary group of students in my lab tested this hypothesis and conclusively demonstrated that this model was incorrect. I provide a summary of our results with emphasis placed on contributions made by students.<sup>b</sup>*

In the winter of 2015, a brilliant student from the Northern Alberta Institute of Technology (NAIT) approached me looking for opportunities to do research during the spring and summer terms. Eduardo Reyes Serratos had taken my Applied Genetics class and I knew his tremendous potential. A few weeks later, I assembled a [group of 6 students](#) and received a research grant to prepare a project for the iGEM 2015 competition in Boston. Three of the students, including Eduardo, were so pumped by the experience at Massachusetts Institute of Technology (MIT) that upon arriving home that November they requested to continue their research involvement in my lab. At the time, the structural biology scientific community was trying to decipher the super structure of the HIV matrix (MA) shell and I challenged my students with this unsolved computational biology problem.

duce experimentally determined results, namely the flat [2] and the cylindrical [5] configurations of the MA shell. With some basic python scripting and simple fundamental trigonometry, we finished this part of the project in a few weeks (Figure 2).

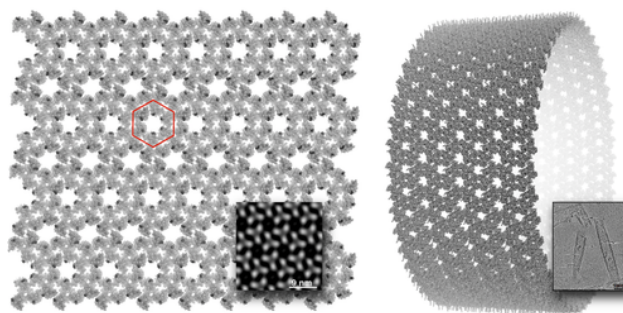


Figure 2: Flat and cylindrical hexagonal arrangements of the MA shell [2, 5] supporting these configurations. A hexagon is shown in red. Hexagons are permissive in flat (left) and cylindrical (right) arrangements of the HIV MA trimers.

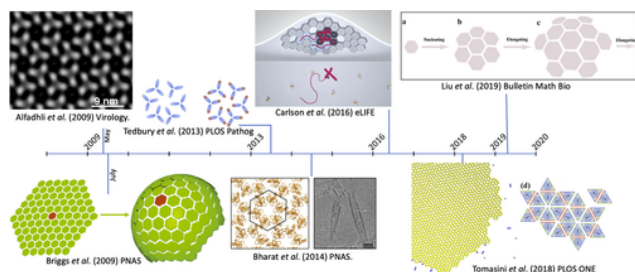


Figure 1: Key Developments in the elucidation of the HIV MA shell superstructure and its impact on the field.

An important key piece of evidence came from work performed by Alfadhli et al [2]. This study demonstrated that HIV MA trimers would arrange themselves in a hexagonal pattern if purified MA trimers were on a flat surface. Shortly thereafter, researchers around the world made the assumption that the structural configuration of the HIV spherical shell was hexagon-based, as shown in a figure published by Briggs et al [3]. A selection of studies [4–8] that were impacted by this hexagon-based model is shown in Figure 1.

My team of students attempted to reconstruct this 3-dimensional model using X-ray crystallography MA structures [9, 10]. Our first objective was to repro-

Our next objective was to assemble a sphere made from these hexagons. We learned, after many attempts, that the configuration was mathematically impossible. In fact, this geometrical fact had been discovered in 1758 by Leonhard Euler [11]. With his famous equation,  $F + V - E = 2$ , he demonstrated that a regular hexagon sphere is not possible (Figure 3).

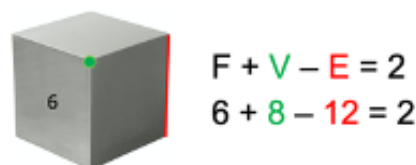


Figure 3: A cube follows Euler's equation. If we add the total number of faces ( $F$ ) to the total number of vertices ( $V$ ) and subtract the total number of edges ( $E$ ), the answer is always 2. This is true for any convex polyhedron and is false if a hexagon is used in the formula.

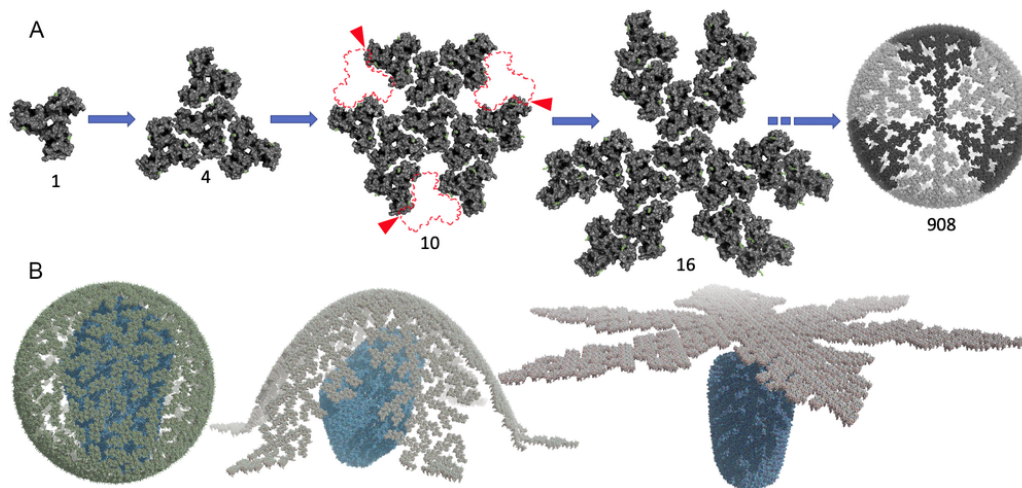


Figure 4: Construction of the HIV MA shell. (A) At 10 trimers, it is not possible to close the hexagons (red arrows and highlighted areas). Doing so results in over imposed trimers. (B) New HIV MA shell models and their putative transitions from sphere to flat. The HIV capsid is shown in blue.

My lab rediscovered this principle and applied this math to the 3-dimensional structure of the HIV MA shell to conclusively demonstrate that the established dogma for the superstructure of the HIV MA shell was incorrect [1]. We then proceeded to create a new model of the MA shell that would respect the geometrical restrictions imposed by the curve of a sphere. Using more [sophisticated math](#) applied by my student Weijie Sun, we followed a simple principle (Figure 4A). Starting from a single trimer resting inside a sphere, we added MA trimers wherever there was space. We built over 10,000 possible structures ranging in diameter from 100 to 200 nm. All structures followed the same general configuration. Adjacent branches of trimers would bend around the spherical surface but would never reconnect. This resulted in a shaped that resembled a flower with 6 petals, mathematically referred to as a 6-lune hosohedra (Figure 4B).

This novel structure led us to predict a new mechanism of viral entry and perhaps viral assembly. Our institute published a [story](#) shortly after to celebrate the achievement of these students.

## Notes

- a. Email: marcelo@ualberta.ca
- b. Original version of this article is Ref. [1]

## References

- [1] Sun, W., Reyes-Serratos, E., Barilla, D., Santos, J. R. L., Bujold, M., Graves, S., and Marcet-Palacios, M., *PLoS One* **14** 11 (2019) e0224965
- [2] Alfadhli, A., Barklis, R. L., and Barklis, E., *Virology* **387** 2 (2009) 466-472
- [3] Briggs, J. A., Riches, J. D., Glass, B., Bartonova, V., Zanetti, G., and Krausslich, H. G., *Proc Natl Acad Sci U S A*, **106** 27 (2009) 11090-11095
- [4] Tedbury, P. R., Ablan, S. D. and Freed, E. O., *PLoS Pathog* **9** 11 (2013) e1003739
- [5] Bharat, T. A., Castillo Menendez, L. R., Hagen, W. J., Lux, V., Igonet, S., Schorb, M., Schur, F. K., Krausslich, H. G. and Briggs, J. A., *Proc Natl Acad Sci U S A* **111** 22 (2014) 8233-8238
- [6] Carlson, L. A., Bai, Y., Keane, S. C., Doudna, J. A. and Hurley, J. H., *Elife* **5** (2016)
- [7] Tomasini, M. D., Johnson, D. S., Mincer, J. S. and Simon, S. M., *PLoS One* **13** 4 (2018) e0196133
- [8] Liu, Y. and Zou, X., *Bull Math Biol* **81** 5 (2019) 1506-1526
- [9] Hill, C. P., Worthylake, D., Bancroft, D. P., Christensen, A. M. and Sundquist, W. I., *Proc Natl Acad Sci U S A* **93** 7 (1996) 3099-3104
- [10] Saad, J. S., Loeliger, E., Luncsford, P., Liriano, M., Tai, J., Kim, A., Miller, J., Joshi, A., Freed, E.O. and Summers, M. F. *J Mol Biol* **366** 2 (2007) 574-585
- [11] Euler, L., *Novi comm. acad. scientiarum imperialis petropolitanae* **4** 109-160 (1758) 1752-1753

# Molecular modeling of chlordecone interactions with acidic activated carbons

Kenia Melchor Rodríguez<sup>a1</sup>, Juan José Gamboa Carballo<sup>1</sup>, Anthuan Ferino Pérez<sup>1</sup>, Nady Passe-Coutrin<sup>2</sup>, Sarra Gaspard<sup>2</sup>, and Ulises Jáuregui Haza<sup>3</sup>

<sup>1</sup>Inst. Superior de Tecnologías y Ciencias Aplicadas (InSTEC) and Univ. de La Habana, Cuba

<sup>2</sup>Laboratoire COVACHIM M2E, Université des Antilles, Pointe à Pitre, Guadeloupe

<sup>3</sup>Inst. Tecnológico de Santo Domingo (INTEC), República Dominicana

*We use computational chemistry tools for describing chlordecone interactions with acidic surface groups onto activated carbons (AC), for understanding the adsorption process of pesticide on AC.*

The French departments, Martinique and Guadeloupe, in order to prevent the propagation of the banana weevil (*Cosmopolite sordidus*), which attacks the roots of the banana tree, extensively used chlorinated pesticides, such as chlordecone (CLD), until the beginning of the 1990s, resulting in the contamination of soil and surface waters. Recent studies has demonstrated that CLD, has a long-range environmental transport, to lead to significant adverse effects on human health and/or the environment. In 2009, CLD was included in the Stockholm Convention on Persistent Organic Pollutants, which bans its production and use worldwide. To limit CLD exposure of Guadeloupe and Martinique population, drinking water and other production plants has been equipped with activated carbon filter. However, the adsorption process onto activated carbon is a very complex phenomenon driven by multiple factors that range from chemical composition to textural properties of the AC. In fact, the influence of surface groups (SG) content over adsorption properties has been reported and studied to some extent both theoretically and experimentally for AC.

In the present work, the interactions between CLD and acidic surface groups on AC are evaluated under different pH and solvation conditions, considering energetic and geometrical aspects of CLD-SG aggregates, in order to better understand the adsorption process on AC.

## Systems under study

The coronene has been chosen as AC computational model [1–4]. The edge of coronene has been modified by carboxyl and hydroxyl groups, and it chemical modifications to obtain the oxygen containing models of AC at different pH conditions. The models provide both, the aromatic character and the SGs at the edges of ACs (Fig. 1). CLD and its *gem*-diol form, also known as chlordecone hydrate (CLDh) were modeled, because at a pH > 9, CLD exist in CLDh form [2, 4].

On the other hand, the maximum water molecules number included in the calculations was set to three, in order to study solvation process, since the adsorption of CLD onto AC occurs from aqueous solution.

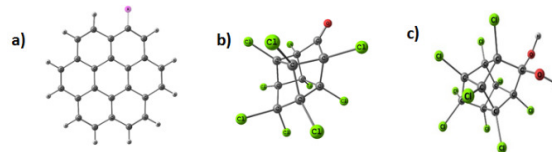


Figure 1: a) AC model consisting on coronene and its oxidized forms:  $X = H$  (Coronene),  $\text{COOH}$ ,  $\text{COO}^-$ ,  $\text{OH}$ ,  $\text{O}^-$ ; b) CLD and c) CLDh.

## Computational methods and procedures

The general methodology employed consists of two main steps: first, the semiempirical Minima Multiple Hypersurface (MMH) methodology is utilized to explore the interactions space of the CLD and CLDh with the SGs-AC; second step, the selected distinctive minima structures obtained from MMH are re-optimized using Density Functional Theory (DFT) and the geometries and electronic structure are treated using Quantum Theory of Atoms in Molecules (QTAIM) to more accurately describe the interactions types [4]. MMH calculations were carried out by MOPAC 2016 and using the semiempirical Hamiltonian PM7. DFT and QTAIM were performed by Gaussian09.

## CLD interaction with SG-AC

Three distinctive interaction types were obtained as result of MMH calculations, see Fig. 2. The first interaction type was predominant and it was observed between the chlorine atoms of CLD and CLDh with the  $\pi$ -cloud of coronene, indicating a relatively weak interaction (Fig. 3a). The bonding distance was in the range of 2.3 and 3.0 Å, suggesting van der Waals interactions between Cl atoms of CLD and CLDh and the planar configuration of coronene molecule. In fact, QTAIM results showed that the dispersive interactions are mainly due by van der Waals forces between chlorine atoms of pesticide and the graphitic surface in AC [2].

As a second interaction type, a donor-acceptor interaction can be described between the negatively charged oxygen of surface groups ( $\text{COO}^-$  and  $\text{O}^-$ ) and electronically deficient carbonyl carbon of chlordecone:  $\text{O}^- \cdots \text{CO}$  (Fig. 3b). This interaction has not been pre-

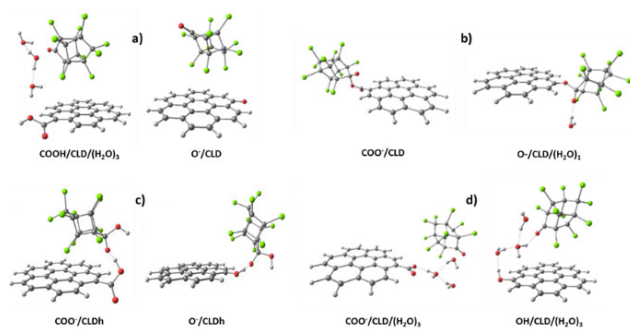


Figure 2: Distinctive interaction types of CLD and CLDh with the acidic surface groups onto AC. a)  $\text{Cl} \cdots \pi$ -cloud interaction, b)  $\text{O}^- \cdots \text{CO}$  interaction and c)  $\text{C} - \text{OH} \cdots \text{O}^-$  interaction. Note in d) how water molecules network are between CLD and SGs.

viously described and it was observed only at slightly acidic and neutral pH conditions and is only present in charged systems. QTAIM calculations showed a few structures with  $\text{O}^- \cdots \text{CO}$  interactions with weak to strong covalent bonds. This ratifies the idea of chemical sorption at slightly acidic and neutral pH conditions and reinforced the experimental results [2].

The third interaction type consists on an electrostatic interaction between the di-alcohol group of CLDh molecule and the negatively charged oxygen of SGs, represented as  $\text{C} - \text{OH} \cdots \text{O}^-$  (Fig. 3c). QTAIM results confirmed this kind of interaction, but is important to explain that this interaction was found only at vacuum, (absence of water molecules). The interaction of CLDh with the acidic SG is favored through a dispersive (governed by van der Waals interactions of chlorine atoms of CLDh with the graphitic surface) and electrostatic interactions (H-bonding interactions of CLDh with SGs on AC in presence of water molecules [4].

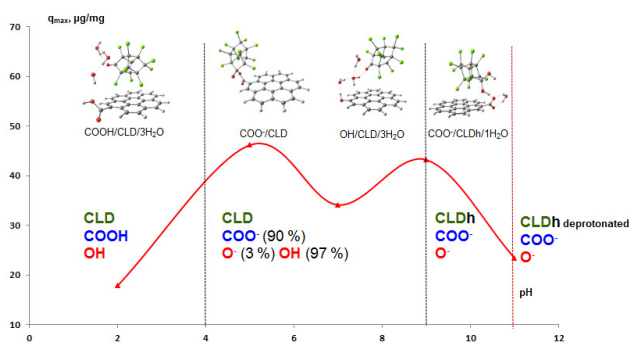


Figure 3: Relationship between experimental and theoretical results. The red line represents the absorption capacity of CLD on BagP0.5 with pH. (BagP0.5 is an AC obtained from sugarcane bagasse collected in Guadeloupe)

The formation of H-bonds and H-bond clusters of water molecules, when one or two molecules of water are close to the interaction site, has been also described through  $\text{C} - \text{OH} \cdots \text{OH}_2$  hydrogen bonds (Fig. 3d).

The DFT optimization of the selected structures using CAM B3LYP/6-31+G(d,p) and M06-2X functional, showed in most of the cases that the structures conserved their geometry and the interaction type.

Taking into account the association energy,  $\Delta E_{Assoc}$ , of the  $\text{SG/CLD}/(\text{H}_2\text{O})_{n=1-3}$  and the  $\text{SG/CLDh}/(\text{H}_2\text{O})_{n=1-3}$  systems, it was confirmed that there is no significant difference between obtained values of  $\Delta E_{Assoc}$  at acidic, neutral and basic pH.

## Summary

Theoretical and experimental results are in agreement [1, 2, 4], suggesting that the mechanism of adsorption of CLD on acidic surface groups of activated carbons at  $\text{pH} \approx 5 - 7$  occurs through a chemisorption and a physisorption and at basic pH conditions through a physisorption. However, at  $\text{pH} \approx 2 - 4$  and  $\text{pH} > 9$ , a very little dependence of the adsorption process of CLD on the SGs composition is observed (Fig. 3). The  $-\text{COO}^-$  surface group have a higher influence over the contaminant adsorption than  $-\text{O}^-$  group, confirming that an increase in carboxylic SG content is expected to enhance CLD adsorption onto AC, which are in agreement with experimental results [1].

## Notes

a. Email: keniamr@instec.cu

## References

- [1] A. Durimel, S. Altenor, R. Miranda-Quintana, P. Couespel Du Mesnil, U. Jáuregui-Haza, R. Gadiou and S. Gaspard, *Chemical Engineering Journal*, **229** (2013) 239-349
- [2] J.J. Gamboa-Carballo, K. Melchor-Rodríguez, D. Hernández-Valdés, C. Enríquez-Victorero, A.L. Montero-Alejo, S. Gaspard and U. Jáuregui-Haza, *Journal of Molecular Graphics and Modelling*, **65** (2016) 83-93
- [3] C. Enriquez-Victorero, D. Hernández Valdés, A.L. Montero Alejo, A. Durimel, S. Gaspard and U. Jáuregui-Haza, *Journal of Molecular Graphics and Modelling*, **51** (2014) 137-148
- [4] K. Melchor-Rodríguez, J.J. Gamboa-Carballo, A. Ferino-Pérez, N. Passé-Coutrin, S. Gaspard and U. Jáuregui-Haza, *Journal of Molecular Graphics and Modelling*, **81** (2018) 146-154

# Small bubbles and bubble bags: a scientific knowledge valorisation

David Fernandez Rivas<sup>a1</sup>

<sup>1</sup>Mesoscale Chemical Systems Group, MESA+ Institute, and Faculty of Science and Technology, University of Twente, Enschede, Netherlands

*This is the story of a PhD project that turned into a spin-off company on ultrasonic cleaning and advanced chemical processes. The basics of sonochemistry and process intensification are also introduced.*

As a scientist trained in Cuba, the word *entrepreneur* had a different meaning to me than for colleagues abroad. Its accurate interpretation is debatable, and it is beyond the scope of this work. Thus, let it be an individual with the drive to bring knowledge or a given solution to the broader society, with or without financial or altruistic motivations. I want to share some of my steps to valorise results obtained during my PhD project. My hope is to illustrate, and inspire other scientists to consider the possibility to start their own business, join a start-up, or transfer their experience and knowledge in the most efficient way to society.

## Microfluidics and Ultrasonic Sonochemistry

Microfluidics can be roughly understood as devices and methods to control and manipulate fluids at length scales below the millimetre, and flow rates not exceeding  $\sim 1 \text{ mL} \cdot \text{min}^{-1}$ . Ultrasonic sonochemistry encompasses the chemical and physical effects caused by applying ultrasound to multiphase systems. Cavitation, the growth and implosion of gas/vapor bubbles in a liquid, arises mostly from the collapse of bubbles in the sonicated liquid [1].

The implosion of bubbles enhance numerous chemical reactions. Each bubble functions as a microreactor with a high-energy environment (temperatures of 5000 °C and pressures of 2000 atm), which in turn produces a plethora of excited chemical species. My PhD's main task was to improve the energy efficiency of sonochemistry with microreactors, and while I was relatively familiar with microfluidics, [2, 3], the sonochemistry community did not think it possible.

## Scaling Up Cavitation

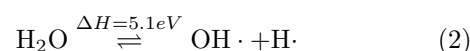
This story started by demonstrating how a significant gain in efficiency is obtained when the location of the nucleation of bubbles, which later cavitate due to ultrasound, is accurately controlled [4]. Such feat was achieved with silicon surfaces on which pits were micro-machined to entrap gas. Upon ultrasonic excitation, the entrapped gas bubble emits a stream of chemically active microbubbles at powers well below the required in conventional reactors.

The lack of reproducibility and very low energy efficiency values of  $X_{US} \sim \mathcal{O}(10^{-6})$  (see Eq. (1)), are the main cause of a poor adoption of the “green” advan-

tages of sonochemistry by the chemical industry.

$$X_{US} = \frac{\Delta H(\Delta N_{rad}/\Delta t)}{P_{US}} \quad (1)$$

where  $\Delta H$  is the energy required for the formation of OH· radicals, which is equal to the enthalpy of formation of the chemical reaction with a value of 5.1 eV per molecule:



$P_{US}$  is the electric power absorbed by the transducer which can be obtained from the measured voltage, current and their phase difference.

Such control over the spatial distribution of cavitation, and the actual volume of liquid exposed to sonochemical effects, enabled us to demonstrate that there was a possibility to number up and scale up the original microreactor into a novel type of sonochemical reactor: the Cavitation Intensifying Bags, CIB [5, 7, 6]. The main contribution of our design, was later interpreted as a process intensification approach by changing the *structure* of the reactor walls (see Figure 1).

## Entrepreneur or academic?

About a year before finalising my PhD, I was working with a friend and scientific collaborator in the lab. We had published some work on the potential uses of the microreactor introduced above, for removing bacteria biofilm from glass and other materials. In a classical “Friday afternoon” experiment, we coloured a contact lens with a permanent marker and exposed its surface to the ultrasonic bubbles. After seeing that without any detergent the ink was removed, no damage to the lens was made, and consulting with our supervisors, we knew we were onto something good.

The University of Twente (UT), has a motto that translates as: *the entrepreneurial university*. For years I biked in front of that banner, without paying much attention to its meaning. But with the uncertainty of what would happen after my PhD was over, and the exciting results, we founded BuBclean ([www.bubbclean.nl](http://www.bubbclean.nl)) and became entrepreneurs.

With the support of the UT's valorisation office, we applied for a patent, took a couple of courses as go-to-market training, and got exposed to the “real world” outside the university walls. We applied to a small government subsidy that allowed us to get our first

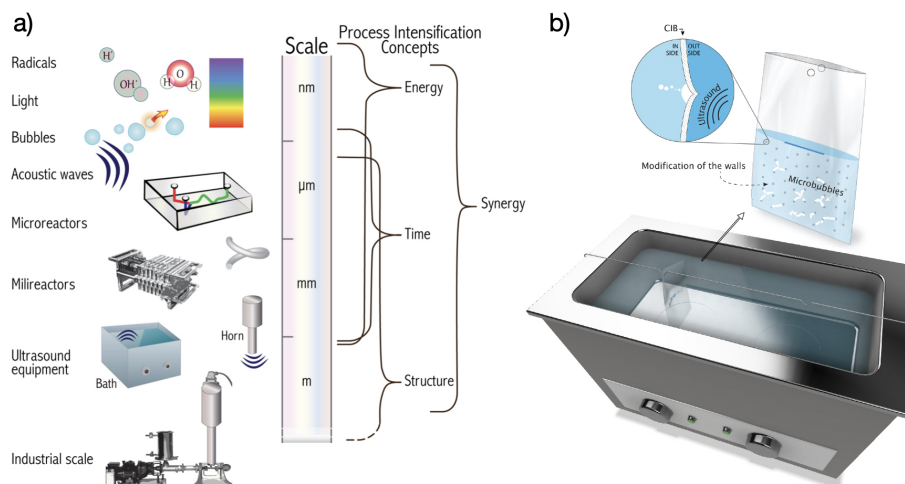


Figure 1: a) Terms and concepts with corresponding relative sizes of the items described in this work, linked to process intensification concepts [9] b) The Cavitation Intensifying Bag CIB (top) is positioned inside an ultrasonic bath (bottom) above one of its transducers (Copyright 2013, with permission from Elsevier [7]) .

customers, mainly from consultancy services. In parallel, we designed, manufactured and started to commercialise what is now the BuBble Bags [10]. We even had to develop a method to convince customers on the advantages of using our product [8] (see Table 1).

Case	Factor	Normal	CIB	IF
Jeweller	Time [min]	10	2.5	240
	Volume [L]	3	0.05	
3D printed	Time [min]	8	1	16
	Volume [L]	100	50	

Table 1: The superiority of Cavitation Intensification Bags evidenced by larger Intensification Factor (IF) values in ultrasonic cleaning [8].

## Conclusions and recommendations

To those who want to embark on the fascinating path of commercialising one scientific idea: it is better to “fail fast” and learn, than to wonder what might have been. If you have no “idea”, you can join an existing start-up. In some countries creating a company might be complicated, but entrepreneurial attitudes within existing organisations is an option (often termed “intrapreneur”). The biggest challenge is building the right team; therefore, skills and personalities should be complemented.

Lastly, persistence is your best ally if you really believe in your dream, and you must be flexible to adapt to changing priorities. It is wise to have a strategy, both for the company and for your personal situation, e.g. have a back up plan in case the entrepreneurship fails may make the leap more comfortable for some. I had the privilege to balance my academic career and entrepreneurial ambitions, and I know this is difficult to replicate; however, it is worth trying it.

## Notes

a. Email: d.fernandezrivas@utwente.nl

## References

- [1] Rivas, D. F. et al., Merging microfluidics and sonochemistry: towards greener and more efficient micro-sono-reactors, *Chemical communications*, **48** 89 (2012) 10935-10947
- [2] Rivas, D. F., Microfluidos: ¿cuánto hay de nuevo?, *Revista Cubana de Física*, **25** 2B (2008) 142-149
- [3] Rivas, D. F., Microfluidos: nuevas fronteras, *Revista Cubana de Física*, **28** 1 (2011) 60-67
- [4] Rivas, D. F. et al., Efficient sonochemistry through microbubbles generated with micromachined surfaces, *Angewandte Chemie International Edition*, **49** 50 (2010) 9699-9701
- [5] Verhaagen, B. et al., Scaled-up sonochemical microreactor with increased efficiency and reproducibility, *ChemistrySelect*, **1** 2 (2016) 136-139
- [6] Gomes, F. et al., Is reproducibility inside the bag?, *Ultrasonics sonochemistry*, **40** Part B (2018) 163-174
- [7] van Zwieten, R. et al., Emulsification in novel ultrasonic cavitation intensifying bag reactors, *Ultrasonics sonochemistry*, **36** (2017) 446-453
- [8] Rivas, D. F. et al., Evaluation method for process intensification alternatives, *Chemical Engineering & Processing-Process Intensification*, **123** (2018) 221-232
- [9] Rivas D. F. and Kuhn S, *Synergy of Microfluidics and Ultrasound*, In: Colmenares J. and Chatel G. (eds) *Sonochemistry. Topics in Current Chemistry*, Springer (2017)
- [10] BuBble bags video [https://youtu.be/1\\_0QT1qrQ-w](https://youtu.be/1_0QT1qrQ-w), in Youtube

# A quantum vaccinomics approach to vaccine development

José de la Fuente<sup>a1,2</sup>, Marinela Contreras<sup>3</sup>, Sara Artigas-Jerónimo<sup>1</sup>, and Margarita Villar<sup>1,4</sup>

<sup>1</sup>SaBio. Instituto de Investigación en Recursos Cinegéticos IREC-CSIC-UCLM-JCCM, Ronda de Toledo s/n, 13005 Ciudad Real, Spain.

<sup>2</sup>Department of Veterinary Pathobiology, Center for Veterinary Health Sciences, Oklahoma State University, Stillwater, OK 74078, USA.

<sup>3</sup>Interdisciplinary Laboratory of Clinical Analysis, Interlab-UMU, Regional Campus of International Excellence Campus Mare Nostrum, University of Murcia, Espinardo, 30100 Murcia, Spain.

<sup>4</sup>Biochemistry Section, Faculty of Science and Chemical Technologies, and Regional Centre for Biomedical Research (CRIB), University of Castilla-La Mancha, 13071, Ciudad Real, Spain.

*A quantum vaccinomics approach was proposed based on the characterization of vector-host-pathogen molecular interactions and the immunological quantum to further advance the design of more effective and safe vaccines*

## Vaccines and the control of infectious diseases

According to the World Health Organization (WHO), vaccines currently prevent between 2 and 3 million deaths and protect many millions more from illness yearly, which supports that it constitutes the most effective preventive intervention to reduce disease, disability, and death from a variety of infectious diseases. Vector-borne diseases (VBD) represent a growing burden for human and animal health worldwide and vaccines are the most effective and environmentally sound approach for the control of vector infestations and pathogen infection and transmission [1]. However, the development of effective vaccines for the control of VBD requires new experimental approaches for the identification of protective antigens and vaccine formulation [2].

## From quantum physics to quantum vaccinomics

Biological systems are dynamical with constant exchange of energy and matter with the environment in order to maintain the state of non-equilibrium characteristic of living systems. Quantum biology is supported by several mechanisms within living cells that operate under non-trivial features of quantum mechanics such as quantum tunneling, which has been proposed to be involved in DNA mutation biological process [3]. Recent evidences showed that living organisms may depend on the dynamics of small number of molecules such as proteins that are well localized (at nanometer scale) and operating over short time periods (in picoseconds), which support that non-trivial quantum mechanical processes play an important role in living systems before decoherence induced by surrounding environment can wash them out. Despite the fact that area of quantum biology related to DNA mutation requires experimental evidence that are difficult to obtain, it is accepted that quantum dynamics within living systems has been subjected to optimizing evolution, and life has learned to manipulate these

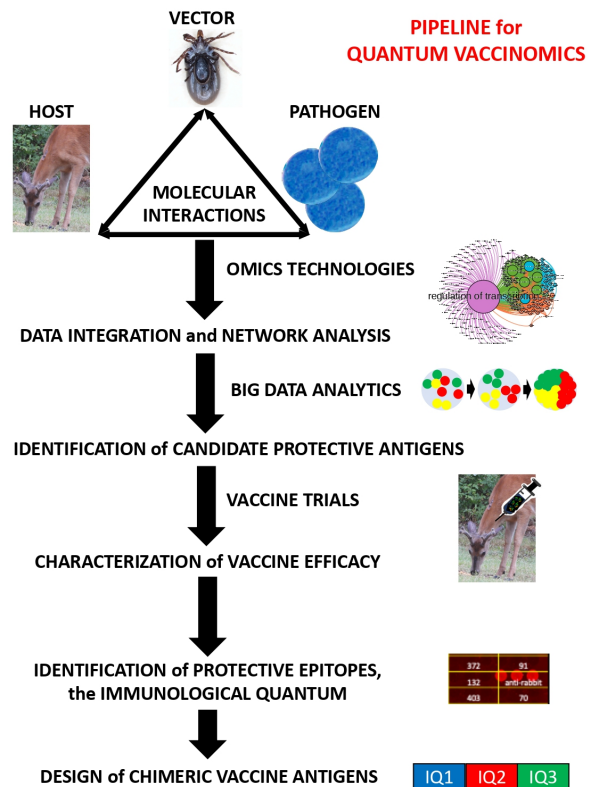


Figure 1: Proposed pipeline for quantum vaccinomics. We thank Katherine M. Kocan (OSU, USA) for the host, vector and pathogen images.

quantum systems to its advantage in ways that need to be approached by future quantum biology studies [3]. The immune system contains random processes such as the direct correlation between atomic coordination and peptide immunogenicity that support quantum immunology [4].

The characterization of vector-host-pathogen molecular interactions and vaccinomics have been proposed as approaches for the development of vaccines for the control of VBD [5]. Then, based on the Albert Ein-

stein's definition of the photon as a quantum of light, the immune protective epitopes were proposed as the immunological quantum [6]. These facts led to the proposal of quantum vaccinomics as the characterization of the immunological quantum to further advance the design of more effective and safe vaccines [6].

Our proposed pipeline for quantum vaccinomics (Fig. 1) consists of the characterization of vector-host-pathogen molecular interactions using omics technologies combined with multi-omics data integration and network analysis [5]. The role of cell interactome and regulome in vector-host-pathogen interactions is then used in a vaccinomics and Big Data analytics approaches for the identification of proteins playing a central role in the regulation of biological processes and with protective antigen capacity in vaccination trials [5]. The selected proteins are then used in quantum vaccinomics for the identification and characterization of the protective epitopes or immunological quantum (IQ) for the design and production of chimeric protective antigens [6].

### Conclusions

The application of quantum vaccinomics would allow the identification of multiple candidate protective antigens and immunological quantum. The combination of ectoparasite vector-derived with pathogen-derived immunological quantum in designed vaccine chimeric antigens is the basis for developing vaccines effective for the control of vector infestations and pathogen infection/transmission. This methodological approach would allow the development of vaccine formulations for the prevention and control of multiple infectious diseases.

### Notes

a. Email: jose.delafuente@yahoo.com/josedejesus.fuente@uclm.es

### References

- [1] de la Fuente J., Estrada-Peña A., Why new vaccines for the control of ectoparasite vectors have not been registered and commercialized?, *Vaccines* **7** Issue (2019) 75
- [2] de la Fuente J., Controlling ticks and tick-borne diseases...looking forward, *Ticks Tick-Borne Dis* **9** Issue (2018) 1354-1357
- [3] McFadden J., Al-Khalili J., The origins of quantum biology, *Proc Math Phys Eng Sci* **474** 2220 (2018) 20180674
- [4] Germenis A.E., Manoussakis M.N., Antipas G.S.E., The dawn of quantum immunology, *SRL Immunol Immunother* **1** (2018) 003-006
- [5] de la Fuente J., Villar M., Estrada-Peña A., Olivas J.A., High throughput discovery and characterization of tick and pathogen vaccine protective antigens using vaccinomics with intelligent Big Data analytic techniques, *Expert Rev Vaccines* **17** (2018) 596-576
- [6] Artigas-Jerónimo S., Pastor Comín J.J., Villar M., Contreras M., Alberdi P., Viera I.L., Soto L., Cordero R., Valdés J.J., Cabezas-Cruz A., Estrada-Peña A., Fuente J. ,A novel combined scientific and artistic approach for advanced characterization of interactomes: the Akiri/Subolesin model, *Vaccines* **8** (2020) 77

# Gershgorin radii as natural bounds for the correlation energies

A. Odriazola<sup>a1</sup>

<sup>1</sup>School of Electrical, Computer, and Energy Engineering, Arizona State University, Tempe, AZ 85287, USA

*We investigate yet another direct link between linear algebra and electronic structure theory by exploring the usefulness of the Gershgorin theorem in the estimation of the correlation energies of many-particle systems.*

The calculation of the eigenvalues of arbitrary matrices is a routine activity in today's science. However, it is a fundamentally complex problem and, in most cases, a very demanding one from the computational point of view. Therefore, to obtain good estimates of the eigenvalues is of vital importance.

In this work we investigate another direct link between linear algebra and electronic structure theory by exploring the usefulness of the Gershgorin theorem [1] in the estimation of the correlation energies  $E_c$  of many-particle systems. We focus on a particular class of systems, two-dimensional quantum dots (2DQDs), and perform extensive numerical calculations. We find that, indeed, the Gershgorin radii  $R_G$  constitute *natural* bounds for the correlation energies though – unfortunately – very loose bounds.

## The Gershgorin theorem

The most crude estimate of the eigenvalues of a matrix  $A$  is given by the inequality  $\rho(A) \leq \|A\|$ , where  $\rho(A) = \max |\lambda|$  with  $\lambda \in \sigma(A)$ , is known as the spectral radius of  $A$ . This estimate, although useful in many cases, is not very accurate in terms of the location of the eigenvalues of  $A$ . Gershgorin's theorem goes further in this direction. Let us recall:

**Theorem 1** *Let  $A = a_{i,j}$  be an arbitrary  $n \times n$  matrix and let us define the disks  $\mathcal{D}_i$  by  $\mathcal{D}_i = \{z \in \mathbb{C} : |z - a_{i,i}| \leq r_i\}$ , where  $r_i = \sum_{i \neq j} |a_{i,j}|$  with  $1 \leq i \leq n$ . Then*

$$\lambda \in \bigcup_{i=1}^n \mathcal{D}_i \quad (1)$$

*for every eigenvalue  $\lambda$  of  $A$ . Furthermore, if  $S$  is the union set of  $m$  disks which are disjoint from the other  $n - m$  disks, then  $S$  contains exactly  $m$  eigenvalues of  $A$ .*

Now, let us analyze the structure of the Full Configuration Interaction (FCI) matrix but taking into account the definition of the correlation energy  $E_c = E_{gs} - E_{HF}$ . That is, the difference between the total ground-state energy and the Hartree-Fock energy. Fig. 1 shows its general structure. Note that the matrix is Hermitian, therefore only the upper triangle is shown.

It is easy to realize that if (i) we use a Hartree-Fock basis,  $|\Phi_0\rangle = |\text{HF}\rangle$ , and (ii) we apply the Gershgorin Theorem to the first eigenvalue of the FCI matrix (See

$$\begin{matrix} & |\Phi_0\rangle & |S\rangle & |D\rangle & |T\rangle & \dots \\ \langle\Phi_0| & E_0 & \mathbf{0} & \int \Phi_0 \hat{H} D & \mathbf{0} & \dots \\ \langle S| & & \int S \hat{H} S & \int S \hat{H} D & \int S \hat{H} T & \dots \\ \langle D| & & & \int D \hat{H} D & \int D \hat{H} T & \dots \\ \langle T| & & & & \int T \hat{H} T & \dots \\ \vdots & & & & & \ddots \end{matrix}$$

Figure 1: Structure of the full-CI matrix. Singly, doubly, triply, and highly excited determinants are denoted as  $|S\rangle$ ,  $|D\rangle$ ,  $|T\rangle$ , etc.

Fig. 1), then we can associate the correlation energy  $E_c$  to the first Gershgorin radius. That is

$$|E_c| < \sum_{j=1}^{\text{Dim}(D)} D_{1,j}, \quad (2)$$

where we use the shorthand notation  $D$  and  $\text{Dim}(D)$  to denote the submatrix  $\int \Phi_0 \hat{H} D$  and its dimension, respectively. The sum in Eq. (2) runs over all elements of the submatrix  $D$ . Let us recall that, in a scheme of FCI, there is no mixture of HF with excitations higher than  $|D\rangle$ , which means that the higher excitation sectors ( $|T\rangle$ ,  $|Q\rangle$ , etc), contain only null elements.

According to Eq. (2), the (first) Gershgorin radius is a *natural* (mathematical) bound for the (ground-state) correlation energy. However, it cannot be said – a priori – how *tight* this bound is. Therefore, our next steps are 1) to study how the Gershgorin radii depends on the parameters defining our system and, 2) to determine under which conditions – if any – they provide useful estimates of the correlation energies.

## Numerical results

In order to evaluate the quality of the above bounds, we consider a concrete model system. We compute the correlation energy and the first Gershgorin radius,  $R_G$ , of two-dimensional parabolic quantum dots with different number of electrons and different confinements strengths. For the calculation of  $R_G$ , we use our own implementation of a truncated CI scheme (up to the singles-and-doubles excitation level) [2].

The starting point is the Hartree-Fock solution of the problem. Then a basis of functions made up from (i) the Hartree-Fock state,  $|\text{HF}\rangle$ , (ii) one-particle one-hole (1p1h) excitations, that is  $|\sigma\mu\rangle = e_{\sigma}^{\dagger} e_{\mu} |\text{HF}\rangle$ ,

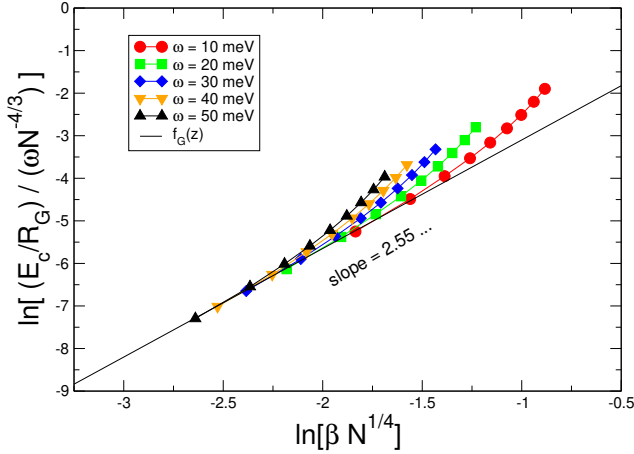


Figure 2: An *approximate* scaling relation of the ratio  $E_c/R_G$  as a function of  $z = \beta N^{1/4}$  (see main text). The deviations observed for large- $N$  systems are a consequence of the basis truncation at double-excitations level.

and (iii) two-particle two-hole (2p2h) excitations, i.e.  $|\sigma\rho, \mu\lambda\rangle = e_\sigma^\dagger e_\rho^\dagger e_\mu e_\lambda |\text{HF}\rangle$ ; is used in order to diagonalize the Hamiltonian. Note that  $e(e^\dagger)$  are the annihilation (creation) operators while  $\sigma < \rho$  are single-particle states above the Fermi level, and  $\mu < \lambda$  are states below the Fermi level. The explicit matrix elements are given in Ref. [2].

We computed values of  $R_G$  of QDs with  $N = 2, 6, 12, 20, 30, 42, 56, 72$  and 90 electrons, and confinement strengths  $\hbar\omega = 10, 20, 30, 40$  and 50 meV. GaAs parameters for the electron effective mass ( $m = 0.067 m_0$ ) and dielectric constant ( $\epsilon = 12.8$ ) were used in the calculations. Notice that all the systems considered here are closed-shell quantum dots with ground-state angular momentum and spin quantum numbers  $L = S = 0$ . As a reference, we also compute values of  $E_c$  based on an accurate Variational Monte Carlo (VMC) approach [3, 4].

We compared the VMC-based reference values of  $E_c$  to the corresponding Gershgorin radii and we found similar qualitative trends, i.e., in a logarithmic scale, the values of both  $E_c$  and  $R_G$  show a linear dependence on the particle number. In the case of  $R_G$ , we observe a deviation from the linear behavior in the large- $N$  region. Such deviations can be explained as the effects of the truncation of the basis in our CI scheme. The main difference, however, is quantitative:  $R_G$  being about three orders of magnitude larger than the corresponding values of  $E_c$ . This numerical difference makes  $R_G$  useless in terms of chemical accuracy.

Even though the Gershgorin radii do not constitute reasonably tight bounds for the correlation energies of the systems considered, we show that both magnitudes may be related by some kind of *scaling law* of the type reported in previous works [2]. To this end, we assume a relation of the form

$$\frac{E_c}{R_G} \sim (\hbar\omega)^{\alpha_R} N^{\beta_R} f_G(z), \quad (3)$$

where  $\alpha_R$  and  $\beta_R$  are numerical constants, and  $z = \beta N^{1/4}$  is the interaction coupling parameter ( $\beta \propto (\hbar\omega)^{-1/2}$  being the ratio between the Coulomb energy and the harmonic confinement) [2].

From our numerical data we find that, in a logarithmic scale, the scaled ratio  $E_c/R_G$  is a linear function of  $z$ :

$$\ln\left(\frac{E_c/R_G}{\hbar\omega N^{4/3}}\right) \approx a \ln(z) + b, \quad (4)$$

where  $a = 2.55$  and  $b = 0.55$  are obtained from a fit to the small- $N$  systems (see Fig. 2). The expression in Eq. (4), after some algebra, can be written in a compact form  $E_c = K R_G$ , where the coefficient  $K$  is a function of  $N$  and  $\hbar\omega$ :

$$K(\hbar\omega, N) = e^b (\hbar\omega)^{\frac{2-a}{2}} N^{\frac{3a-16}{12}}. \quad (5)$$

The scaling law shown in Fig. 2 was found “empirically”, and a rigorous proof of this relation is yet to be found. However, improved values of all numerical parameters can be achieved by including larger data sets.

## Conclusions

Our results imply that, (i) in the first approximation the first Gershgorin radius does not provide a tight enough bound for the correlation energy of 2DQDs, but (ii) both quantities can be numerically related by means of scaling law. These conclusions apply only to a particular class of systems (2DQDs) and the situation can differ in different systems. This possibility, in our opinion, is what makes the problem worth exploring: the promise of finding – with a highly parallelizable recipe – good estimates of the eigenvalues without diagonalising the matrix, even when the so-called chemical accuracy requires this bounds to be extremely sharp.

## Notes

a. Email: aodriazo@asu.edu (On leave: *mere association*)

## References

- [1] S. Gershgorin, Über die Abgrenzung der Eigenwerte einer Matrix, *Izv. Akad. Nauk. USSR Otd. Fiz.-Mat. Nauk (in German)*, **6** (1931) 749
- [2] A. Odriazola, A. Delgado and A. Gonzalez, *Phys. Rev. B*, **78** (2008) 205320
- [3] A. Harju, *J. Low Temp. Physics*, **140** (2005) 181
- [4] A. Odriazola, *Scaling Approaches to Quantum Many-Body Problems*, Tampere University of Technology. Publication Vol. 1525 (2017)